Life Sciences in Space Research 47 (2025) 105–123

Contents lists available at ScienceDirect

Life Sciences in Space Research

journal homepage: www.elsevier.com/locate/lssr

Towards supervisory Model Predictive Control for circular life support systems in long-term space missions

Gionata Cimini [a,*], Marco Gatti [b], Daniele Bernardini [a], Alberto Bemporad [c], Chloé Audas [d], Claude-Gilles Dussap [e]

[a] ODYS S.r.l., Milan, Italy
[b] EnginSoft S.p.A., Bergamo, Italy
[c] IMT School for Advanced Studies Lucca, Lucca, Italy
[d] European Space Agency, Noordwijk, The Netherlands
[e] Université Clermont Auvergne, Clermont-Ferrand, France

ARTICLE INFO

Keywords:
Regenerative Life Support System
Long-term space mission
Circular systems
Nonlinear Model Predictive Control
Supervisory control
Constrained optimization

ABSTRACT

Regenerative Life Support Systems (LSS) fulfill the essential functions for human survival in space, such as atmosphere revitalization, water recovery, food production, and waste management, and are crucial for long-term space missions where the resupply of resources from Earth is not feasible or reliable. Operating a regenerative LSS poses several challenges, mainly related to its complexity, efficiency, and reliability. A set of heterogeneous subsystems involving mechanical, chemical, biological, and energetic processes has to be optimally coordinated in order to meet the requirements on mass, power, crew time, safety, reliability, sustainability and efficiency. In this paper, we address these challenges by proposing a supervisory control layer based on a nonlinear and time-varying Model Predictive Control (MPC) approach. The mathematical framework for deriving the prediction model addresses generic regenerative LSS. The MELiSSA (Micro-Ecological Life Support System Alternative) project developed by the European Space Agency is used here as the test case. For the first time, a complete dynamical model including all the MELiSSA compartments connected on all the phases (solid, liquid, gas) is derived, simulated, and controlled by a supervisory MPC. The design of such a controller follows a large set of requirements pre-defined by the MELiSSA project. Results on a mission lasting 14 weeks, which also includes a system failure scenario, are reported and evaluated for a specific MELiSSA network architecture.

1. Introduction

Environmental control and life support systems for space applications are complex systems designed to provide astronauts with the necessary resources, environmental conditions, and safety measures to support human life during space missions. These systems are crucial for maintaining astronaut health, comfort, and safety in the challenging and isolated environment of space. Future human exploration missions beyond low Earth orbit will require the provision of metabolic resources and the management of crew waste in partial or complete autonomy from Earth. This calls for regenerative and circular life support systems, and for robust control strategies to manage resources such as oxygen, water and food while ensuring the health and safety of astronauts (Gitelson et al., 1976; Lasseur et al., 1996; Savage et al., 2001; Nelson et al., 2003; Audas et al., 2022).

One of the main control challenges is the inherent complexity of regenerative Life Support Systems (LSS), which involves multiple dynamical processes with widely different timescales and demands that interact with each other and with the crew. At the physical system level, each process has its own local control goals, which are usually complex enough to require advanced control techniques (Binois et al., 1994; Cornet et al., 2002; Pannico et al., 2022). Taking into account safety, survivability, and regeneration requirements means optimizing the interactions between these processes in an integrated way, building on a hierarchical structure with a *global controller* and several low-level controllers (LLC) (Fulget et al., 1999). A global controller is commonly designed to meet system-wide objectives that involve the coordination of different subsystems, and acts as a supervisor that manipulates references, constraints and more generically parameters

* Corresponding author.
E-mail addresses: gionata.cimini@odys.it (G. Cimini), m.gatti@enginsoft.com (M. Gatti), daniele.bernardini@odys.it (D. Bernardini), alberto.bemporad@imtlucca.it (A. Bemporad), chloe.audas@esa.int (C. Audas), c-gilles.dussap@uca.fr (C.-G. Dussap).

https://doi.org/10.1016/j.lssr.2025.06.001
Received 3 February 2025; Received in revised form 21 April 2025; Accepted 2 June 2025
Available online 18 June 2025
2214-5524/© 2025 Published by Elsevier B.V. on behalf of The Committee on Space Research (COSPAR).

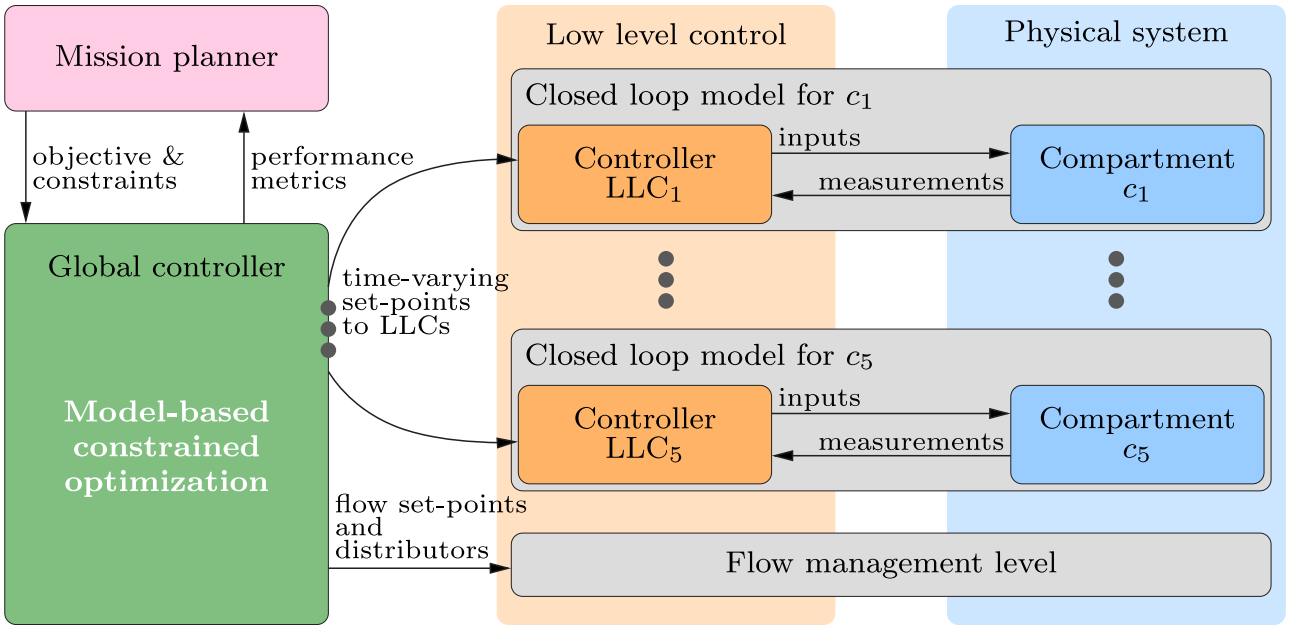

Fig. 1. Hierarchical control structure for a life support system.

of the LLC. The LLC are designed on local objectives relative to the single subsystem operation (in our case the compartments), and are responsible to directly manipulate the actuators. In this work, we focus on the mathematical modeling and control framework for the design of the global controller. Many aspects must be simultaneously considered, such as the need to optimally operate the elements (compartments, storages, distributors, etc.) involved in the loop, the limited degrees of freedom available, the importance of storage management, and the regeneration rate of the resources within the system. Moreover, a reliable supervisory control system for the regenerative LSS has to withstand uncertainties and disturbances, such as equipment failures, microbial contamination, or crew health issues. In light of the challenges that need to be addressed, parallels have been drawn with the control of islanded microgrids (Ciurans et al., 2022).

With these premises, Model Predictive Control (MPC) emerges as an excellent candidate to coordinate a regenerative LSS globally. MPC is one of the most advanced and impactful control methodologies in recent history (Mayne et al., 2018), and by now, it is considered a technology in several fields, such as the chemical industry, automotive or robotics, just to cite a few (Schwenzer et al., 2021; Bemporad et al., 2018; Cimini et al., 2021). Its success is justified by the fact that it is a conceptually simple and universal strategy that enables optimal closed-loop performance of multi-input multi-output systems under constraints. MPC explicitly uses a dynamical model of the system to predict its evolution in time and derives the control law by iteratively solving a finite-time, constrained, optimal control problem along a receding horizon. The control problem is, therefore, formulated as an optimization one. These features perfectly fit in the context of supervisory control of a complex and high-dimensional dynamical system with numerous and conflicting control objectives and constraints. The ability to handle uncertainties and failure conditions is also extremely valuable (Franchi et al., 2018). Additionally, the systematic and adaptable approach of a model-based technique proves helpful in investigating different configurations and ensures the sustainability and success of long-duration missions.

These appealing features are well-known to researchers addressing supervisory control of regenerative LSS, especially when it comes to the MELiSSA (Micro-Ecological Life Support System Alternative) loop (Cornet et al., 2002; Binois et al., 1994; Ciurans et al., 2022). MELiSSA is the leading European project on circular life support systems, led by the European Space Agency. It aims to achieve the highest degree of autonomy in space, i.e. to produce oxygen, water, food, nitrogen and materials for crewed missions to deep space, where otherwise resupply would result in a tremendous cost (Mergeay et al., 1988; Lasseur, 2008). The MELiSSA loop is based on six compartments connected by different transformation processes and constituting a closed-loop system. These compartments include: waste degrading and transformation bioreactors (c_1 and c_2), three compartments concomitantly in charge of oxygen production, water recycling and edible microalgae production completed by a higher plant chamber (c_3, c_{4a} and c_{4b}), and a compartment with human crew as a food, water and air consumer and producer of metabolic waste streams (c_5). The liquefying compartment c_1 decomposes complex wastes (non-edible parts of the plants and crew waste) into simple molecules by anaerobic digestion without producing methane. Moreover, c_1 determines the fraction of organic waste that can be recycled in the rest of the loop. Compartment c_2 converts organic carbon coming from c_1 into carbon dioxide for further utilization in photosynthetic compartments c_{4a} and c_{4b}. Ammonium and minerals coming from c_1 are delivered to c_3, the nitrifying compartment, where ammonium is transformed into a nitrate-rich substrate for higher plants and micro-algae cultivation. Since the beginning of the MELiSSA project, a mechanistic approach has been followed focusing on the modeling of all the processes involved in the loop (Poughon et al., 1999, 2009; Poulet et al., 2020; Thiron, 2020; Dussap et al., 1993). Indeed, previous studies investigated advanced control approaches for the MELiSSA loop (Ciurans et al., 2021; Alemany et al., 2019; Ciurans et al., 2022). These works, however, only addressed the control of specific phases and a restricted set of all the subsystems involved. From a modeling perspective, a comprehensive review of all MELiSSA literature has been recently published (Vermeulen et al., 2023), and a stoichiometric model of the complete MELiSSA loop was developed to describe the static cycling of the chemical elements C, H, O, and N through the MELiSSA compartments.

The work presented in this paper has the ambition of first setting the ground for a generic modeling framework of a complete regenerative LSS loop, including the dynamics of all the compartments connected on all the phases (solid, liquid, gas). Such a mathematical framework is then utilized to derive a full preliminary dynamical model of the specific MELiSSA loop, additionally expanding the chemical setup considered (statically) in Vermeulen et al. (2023) by adding S and P

chemical elements. A supervisory MPC controller is then elaborated and designed, following all the safety, survivability, recycling, and efficiency requirements of the interconnected system, and providing for the first time both a complete dynamical simulation model of the MELiSSA network as well as a supervisory control that is fully aware of all the compartments and phases. The developed closed-loop system is successfully tested in simulation over several scenarios, including also system failures. The results obtained from this closed-loop simulation are very useful not only in the actual design of a supervisory controller but also for rapidly investigating different network architectures and requirements.

The paper is organized as follows: Section 2 introduces the general framework to derive a dynamical model of a regenerative LSS. Section 3 describes the MELiSSA loop and Section 4 the changes adopted to apply the general framework to MELiSSA. Section 5 defines the control requirements and the MPC controller formulation. Simulation results are presented and discussed in Section 6. Finally, concluding remarks are given in Section 7.

2. Mathematical framework for circular life support system modeling

The cornerstone towards mass adoption of advanced control designs, such as MPC, in the context of circular LSS is a systematic procedure to develop control-oriented models that are simple enough to be included in a real-time controller but capture at the same time the dynamics necessary to evaluate safety, recovery, and efficiency metrics. In this section, we propose a rather generic framework for deriving such control-oriented models in the context of flow management for a regenerative LSS. The model will include the chemical transformations of solids, liquids, and gases that occur at different stages of the regenerative LSS, the storage of such components, and their flow across the network. We first define the main components that characterize the regenerative LSS:

- *compartments* refer to the division of network functionalities into separate transformation processes;
- *storages* collect the supplies (e.g., food and water) and the waste produced onboard;
- *distributors* are actuators for the supervisory control that manage the movement of some chemical components from multiple sources to multiple end consumers;
- *flow connections* determine the network architecture, that is, how chemical components can flow among all the aforementioned elements.
- *buffer tanks* are special storages/sinks of specific chemical components meant to guarantee proper operation of the compartments' transformation processes by making up for the lack/excess of such components' availability in the circular system. Buffer tanks are mainly intended for investigating different architectures and their usage should be minimized.

Physical phenomena, such as energy and thermodynamics, are not considered here for several reasons: (*i*) the main requirements of the regenerative LSS can be expressed just in terms of chemical elements conservation, e.g. stoichiometry, (*ii*) the most relevant biological or chemical conversion kinetics are sufficient for a preliminary assessment of the LSS circularity and recycling capabilities, as well as the investigation of different network architectures and the sizing of each network element, (*iii*) the readiness level of the compartments' mechanistic models can be heterogeneous, (*iv*) the physical transformation unit and its low-level control, see Fig. 1, can be expressed with a stoichiometric model assuming optimality of operation.

We then aim at deriving a global model in the form:

$$\frac{\mathrm{d}x(t)}{\mathrm{d}t} = f_x(x(t), u(t), \theta(t)) \tag{1}$$

where $x(t) \in \mathbb{R}^{n_x}$ are the system states, $u(t) \in \mathbb{R}^{n_u}$ are the controlled inputs or manipulated variables, $\theta(t) \in \mathbb{R}^{n_\theta}$ are the exogenous parameters that affect the system dynamics, and $f_x(\cdot)$ is a nonlinear function. The model is presented in its state-only form, because there is not yet an interest into defining measurements that will be available in the real system. As the research progresses, output equations will be considered. The framework is likely to be used in contexts where the maturity of the research on the internal dynamics of compartments is possibly at an early stage, and so is the network architecture; therefore, our main focus is the modularity and flexibility of the formulation. In Section 4, we will then utilize the tools presented here to derive the mathematical model of one of the LSS architectures investigated in the MELiSSA loop. Denoting by $\mathcal{E}$ the set of network elements, each eth element, $e \in \mathcal{E}$, is defined by the following state vector:

$$x_e(t) = \begin{bmatrix} \widetilde{\boldsymbol{\Phi}}_e(t) \\ V_e(t) \end{bmatrix} = \begin{bmatrix} \widetilde{\sigma}_e(t) \\ \widetilde{\lambda}_e(t) \\ \widetilde{\gamma}_e(t) \\ s_e(t) \\ \ell_e(t) \\ g_e(t) \end{bmatrix}, \quad \forall e \in \mathcal{E}. \tag{2}$$

Unless differently specified, from now on, subscript e will denote a quantity that can be extended to all elements in $\mathcal{E}$ of the network. The overall state vector of the system is $x(t) = (x_e(t))_{e\in\mathcal{E}}$. We denote by $n_{\mathcal{E}}$ the cardinality of $\mathcal{E}$. Let n_s, n_ℓ, and n_g be the number of chemical components considered by the model in the solid, liquid, and gas phases, respectively, and $m = n_s + n_\ell + n_g$. Then in (2) we have that:

- $\tilde{\boldsymbol{\Phi}}_e(t) \in \mathbb{R}^m_{\geq 0}$ is the collection of flows (mol/h) resulting from the chemical reactions happening in network element e, particularized such that $\tilde{\sigma}_e(t) \in \mathbb{R}^{n_s}_{\geq 0}$, $\tilde{\lambda}_e(t) \in \mathbb{R}^{n_\ell}_{\geq 0}$, and $\tilde{\gamma}_e(t) \in \mathbb{R}^{n_g}_{\geq 0}$ collect the flows of the solids, liquids, and gases, respectively.
- $V_e(t) \in \mathbb{R}^m_{\geq 0}$ is the collection of chemical components' volumes (mol) in the network element e, with $s_e(t) \in \mathbb{R}^{n_s}_{\geq 0}$, $\ell_e(t) \in \mathbb{R}^{n_\ell}_{\geq 0}$, and $g_e(t) \in \mathbb{R}^{n_g}_{\geq 0}$ collecting the volumes of the solids, liquids, and gases, respectively.

In other words, $\tilde{\boldsymbol{\Phi}}_e(t)$ captures the dynamics relative to the chemical transformations and $V_e(t)$ the accumulation of the so-produced matter. It is worth noticing that liquid flows and volumes may also contain dissolved gas components and that the sets of cardinality n_s, n_ℓ and n_g are composed by the worst-case collection of all the chemical components that flow in the network.

We also introduce the following notation regarding flow manipulation. Given a flow $z \in \mathbb{R}^n$ and a chemical component χ, dropping here the time t, the network element e and the phase for simplicity, we denote by $i_{z,\chi}$ the index of component χ in array z, and by $y = \chi\{z\}$ a flow $y \in \mathbb{R}^n$ in the same phase as z, resulting from a 0-valued mask applied on all other chemical components of this flow other than χ, i.e. $y_{i_{z,\chi}} = z_{i_{z,\chi}}$ and $y_j = 0$, $\forall j \in \{1, \dots, n\}$, $j \neq i_{z,\chi}$. We instead indicate with $y = z|_{\chi=0}$ the complementary flow $y \in \mathbb{R}^n$, in the same phase as z, and such that $y_{i_{z,\chi}} = 0$ and $y_j = z_j$, $\forall j \in \{1, \dots, n\}$, $j \neq i_{z,\chi}$. It follows that $\chi\{z\} + z|_{\chi=0} \equiv z$ holds. The quantity $z_{[\chi]} \triangleq z_{i_{z,\chi}}$ denotes instead the scalar value of χ in z. Moreover, if z is a liquid flow/volume, then the notation $z^\ell \in \mathbb{R}^{n_\ell}$ and $z^g \in \mathbb{R}^{n_g}$ indicate two liquid flow/volume arrays where all the dissolved gases for the former, and the liquids for the second, have been zeroed, and such that $z^\ell + z^g \equiv z$. Given a generic array $x \in \mathbb{R}^n$ we define the normalization function $\pi(\cdot)$ as $\pi(x) \equiv x/\|x\|_1$.

Analogously to (2), we also introduce the concept of *output flows* (mol/h):

$$\boldsymbol{\Phi}_e(t) = \begin{bmatrix} \sigma_e(t) \\ \lambda_e(t) \\ \gamma_e(t) \end{bmatrix} \tag{3}$$

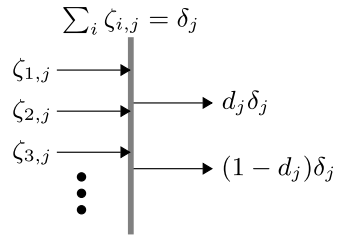

Fig. 2. Diagram of the jth distributor operation, which is controlled by the manipulated variable $d_j \in [0,1]$.

where $\boldsymbol{\Phi}_e(t) \in \mathbb{R}^m_{\geq 0}$ and its components $\sigma_e(t) \in \mathbb{R}^{n_s}_{\geq 0}$, $\lambda_e(t) \in \mathbb{R}^{n_\ell}_{\geq 0}$, and $\gamma_e(t) \in \mathbb{R}^{n_g}_{\geq 0}$ collect the flows in the solid, liquid, and gas phase respectively, representing the matter that leaves network element e.

Typically, the dynamics that involve directly $\boldsymbol{\Phi}_e(t)$, for instance, a valve's opening delay, are much faster than the chemical reactions that take place in the system; we will adopt this assumption in the rest of the paper, although the mathematical framework presented here is general enough to account for the cases in which such phenomena are not negligible. In fact, in such cases, it would be enough to include $\boldsymbol{\Phi}_e(t)$ in the states' array (2). In order to allow this flexibility and ease the notation, the output flows (3) will be nonetheless used as intermediate variables defining the relations at the flow-management level.

A circular system is open to different minimal dynamical state representations. Output flows play a crucial role because (*i*) they are more likely to be in the three phases of the matter for each compartment (being the final product of chemical transformations), (*ii*) for those elements where volumetric dynamics are not explicitly modeled, the output flows correspond to the direct output of the chemical transformations, which translates into:

$$\sigma_e(t) = \tilde{\sigma}_e(t) \text{ if } \dot{s}_e(t) \equiv 0 \tag{4a}$$

$$\lambda_e(t) = \tilde{\lambda}_e(t) \text{ if } \dot{\ell}_e(t) \equiv 0 \tag{4b}$$

$$\gamma_e(t) = \tilde{\gamma}_e(t) \text{ if } \dot{g}_e(t) \equiv 0. \tag{4c}$$

We indicate by $u(t) \in \mathbb{R}^{n_u}$ the set of variables manipulated by the controller, and we distinguish among different categories. The *activity* of the eth network element, namely $\xi_e(t)$, is intended as a scalar that can modulate, possibly in a nonlinear fashion, its production/transformation rate. It is scalar because each compartment, or network element, is characterized by a single stoichiometry but has the flexibility to be either a direct manipulation of physical parameters or a time-varying set-point to the LLC. At the flow management level, we have instead *distributors*, *manipulated flows*, and *buffer tanks*. The distributors are network elements that collect flows coming from multiple sources but strictly at the same chemical phase and route them to two destinations/consumers according to a manipulated ratio. Let $d_j \in [0,1]$ be the manipulated ratio of the jth distributor, $\zeta_{i,j}$ for $i \in \{1,\dots,n_{\zeta_j}\}$, $n_{\zeta_j} > 0$, the incoming flows, and $\delta_j = \sum_{i=1}^{n_{\zeta_j}} \zeta_{i,j}$; then the distributor will route a flow of $d_j\delta_j$ to the first destination, and $(1-d_j)\delta_j$ to the second one. This behavior is summarized in Fig. 2. We note that more complex distribution strategies, which may involve more than two destinations, can be easily implemented with a cascade of distributors, introducing a manipulated variable for each additional distributed flow.

The manipulated flows are scalars that control the output flows of components' mixture in the same phase when the conditions in (4) do not hold, which means that the target element exhibits internal modeled volumes. Let $\kappa^\sigma_e(t)$, $\kappa^\lambda_e(t)$, $\kappa^\gamma_e(t) \in \mathbb{R}$ be the manipulated flows for solids, liquids, and gases, respectively; then we have:

$$\sigma_e(t) = \kappa^\sigma_e(t)\pi(s_e(t)) \text{ if } \dot{s}_e(t) \not\equiv 0 \tag{5a}$$

$$\lambda_e(t) = \kappa^\lambda_e(t)\pi(\ell_e(t)) \text{ if } \dot{\ell}_e(t) \not\equiv 0 \tag{5b}$$

$$\gamma_e(t) = \kappa^\gamma_e(t)\pi(g_e(t)) \text{ if } \dot{g}_e(t) \not\equiv 0 \tag{5c}$$

with $\pi(s_e(t))$, $\pi(\ell_e(t))$ and $\pi(g_e(t))$ the normalized composition of the total solid, liquid, and gas volumes. We note that (4) and (5) completely characterize the output flows' intermediate variables.

We now have all the ingredients to capture the mass flow dynamics of each network element $e \in \mathcal{E}$ by the following dynamical model:

$$\begin{bmatrix}\sigma^\upsilon_e(t)\\ \lambda^\upsilon_e(t)\\ \gamma^\upsilon_e(t)\end{bmatrix} = \upsilon_e\left(\begin{bmatrix}\sigma^\eta_e(t)\\ \lambda^\eta_e(t)\\ \gamma^\eta_e(t)\end{bmatrix}, \xi_e(t)\right) \tag{6a}$$

$$\tau^s_e \frac{\mathrm{d}\tilde{\sigma}_e(t)}{\mathrm{d}t} = \sigma^\upsilon_e(t) - \tilde{\sigma}_e(t) \tag{6b}$$

$$\tau^\ell_e \frac{\mathrm{d}\tilde{\lambda}_e(t)}{\mathrm{d}t} = \lambda^\upsilon_e(t) - \tilde{\lambda}_e(t) \tag{6c}$$

$$\tau^g_e \frac{\mathrm{d}\tilde{\gamma}_e(t)}{\mathrm{d}t} = \gamma^\upsilon_e(t) - \tilde{\gamma}_e(t) \tag{6d}$$

where $\upsilon_e(\cdot)$ is the stoichiometry describing the chemical transformations in the three phases that take place in the compartment, $\sigma^\eta_e(t) \in \mathbb{R}^{n_s}$, $\lambda^\eta_e(t) \in \mathbb{R}^{n_\ell}$, $\gamma^\eta_e(t) \in \mathbb{R}^{n_g}$ the mass flows being transformed by $\upsilon_e(\cdot)$, and $\sigma^\upsilon_e(t) \in \mathbb{R}^{n_s}$, $\lambda^\upsilon_e(t) \in \mathbb{R}^{n_\ell}$, $\gamma^\upsilon_e(t) \in \mathbb{R}^{n_g}$ the result of such transformation, and τ^s_e, τ^ℓ_e, and $\tau^g_e \in \mathbb{R}$ the solid, liquid, and gas time constants relative to the transformation/residency time. We remark that stoichiometries are widely adopted building blocks to represent chemical or biological transformations (Begon and Townsend, 2021).

The model in (6) describes the dynamics of $\tilde{\boldsymbol{\Phi}}_e(t)$ in (2). Note that the manipulated variable $\xi_e(t)$ in (6a) might be not defined for all the network elements.

To derive the expression for $\sigma^\eta_e(t)$, $\lambda^\eta_e(t)$, $\gamma^\eta_e(t)$ we need to introduce $\mu^\sigma_e(t)$, $\mu^\lambda_e(t)$, $\mu^\gamma_e(t) \in \mathbb{R}$ which are scalar quantities close in spirit with the κ's in (5), that can be interpreted as *induced flows* originating by the needs of living beings in e. Due to their nature, the controller has however no authority on them, contrarily to κ's, and they are a function of $\theta(t)$ and, possibly, $x(t)$. Let $\sigma^\iota_e(t) \in \mathbb{R}^{n_s}$, $\lambda^\iota_e(t) \in \mathbb{R}^{n_\ell}$, $\gamma^\iota_e(t) \in \mathbb{R}^{n_g}$ be its input flows of network element e, than we can write:

$$\sigma^\eta_e(t) = \begin{cases}\mu^\sigma_e(t)\pi(s_e(t)) & \text{if } \dot{s}_e(t) \not\equiv 0\\ \sigma^\iota_e(t) & \text{otherwise}\end{cases} \tag{7a}$$

$$\lambda^\eta_e(t) = \begin{cases}\mu^\lambda_e(t)\pi(\ell_e(t)) & \text{if } \dot{\ell}_e(t) \not\equiv 0\\ \lambda^\iota_e(t) & \text{otherwise}\end{cases} \tag{7b}$$

$$\gamma^\eta_e(t) = \begin{cases}\mu^\gamma_e(t)\pi(g_e(t)) & \text{if } \dot{g}_e(t) \not\equiv 0\\ \gamma^\iota_e(t) & \text{otherwise.}\end{cases} \tag{7c}$$

For ease of notation, let us compactly define

$$\boldsymbol{\Phi}^\upsilon_e(t) = \begin{bmatrix}\sigma^{\upsilon\intercal}_e(t) & \lambda^{\upsilon\intercal}_e(t) & \gamma^{\upsilon\intercal}_e(t)\end{bmatrix}^\intercal \tag{8a}$$

$$\boldsymbol{\Phi}^\iota_e(t) = \begin{bmatrix}\sigma^{\iota\intercal}_e(t) & \lambda^{\iota\intercal}_e(t) & \gamma^{\iota\intercal}_e(t)\end{bmatrix}^\intercal. \tag{8b}$$

Lastly, in order to preserve network stability, guarantee robustness against system failures, and more generically conduct research on different architectures, the regenerative LSS is equipped with buffer tanks of specific chemical components. They can be added or removed at prescribed injection points, and clearly each single component at each single injection point represents an independent manipulated variable for the global controller to actuate. We introduce the notation $\langle\chi\rangle_{\vec{e}}(t) \in \mathbb{R}$ for an additive scalar flow (mol/h) of the chemical component χ in the input flows of element $e \in \mathcal{E}$. The collection of all the additive scalar flows in a specific phase is identified by $\sigma_{\vec{e}}(t) \in \mathbb{R}^{n_s}$, $\lambda_{\vec{e}}(t) \in \mathbb{R}^{n_\ell}$, $\gamma_{\vec{e}}(t) \in \mathbb{R}^{n_g}$. For instance, if we enrich an existing network element e with the set of chemical elements $\{\chi_1,\dots,\chi_{n_a}\}$ in the gas phase, let $\mathcal{L} = \{i_{\gamma^\iota_e,\chi_j} \mid j \in 1,\dots,n_a\}$, we have that $\gamma^\iota_e(t) = z(t) + \gamma_{\vec{e}}(t)$ with $z \in \mathbb{R}_{\geq 0}$

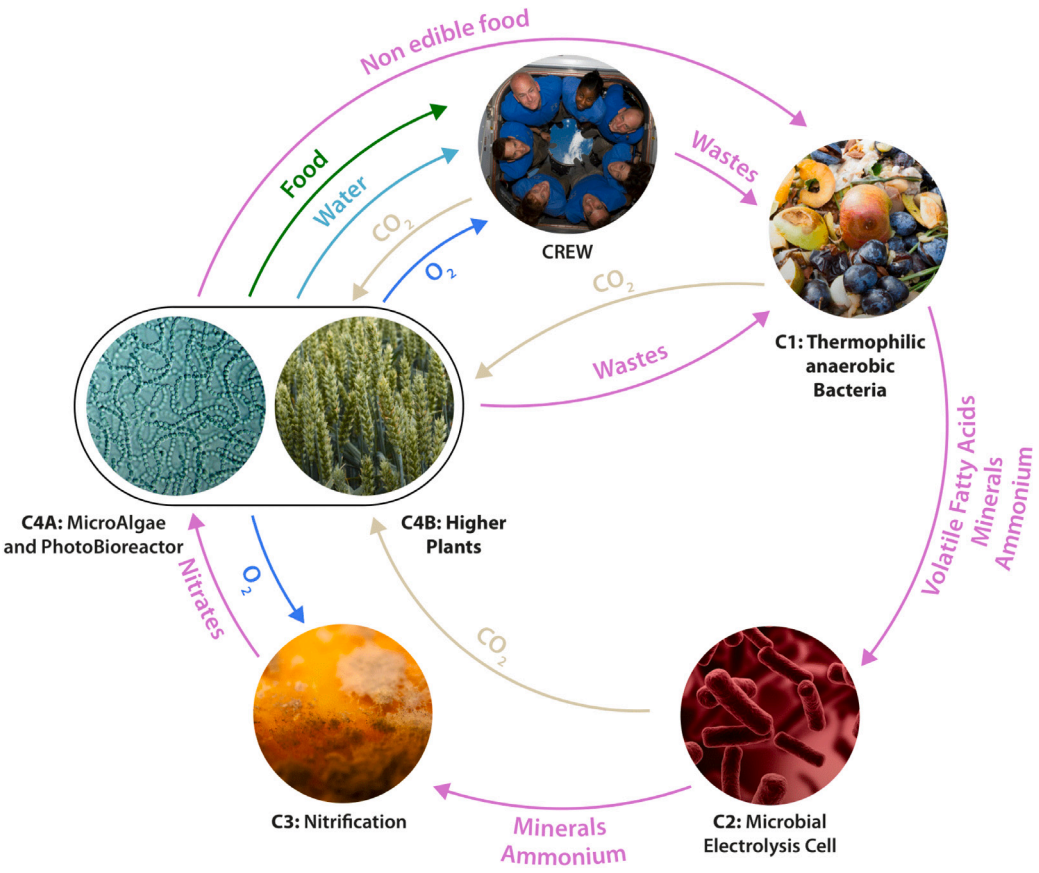

Fig. 3. Concept of the MELiSSA loop: the compartmentalized network.

a flow coming from other elements of the network, and

$$\gamma_{\tilde{e},j}(t) = \begin{cases} \max(-z_j(t), \langle \chi_j \rangle_{\tilde{e}}(t)) & \text{if } \dot{g}(t) \equiv 0 \\ \max(-g_j(t), \langle \chi_j \rangle_{\tilde{e}}(t)) & \text{if } \dot{g}(t) \not\equiv 0 \end{cases}, \forall j \in \mathcal{L} \tag{9a}$$

$$\gamma_{\tilde{e},k}(t) = 0, \quad \forall k \in \{1, \dots, n_g\} \setminus \mathcal{L}. \tag{9b}$$

Please note that the flow in (9) can also be negative, allowing the same manipulated variable to jointly encompass the operation of two separate actuators, a supply tank and a chemical component extraction (e.g., a CO_2 capturing device). The "max" operators ensure the positiveness of volumes and flows that are arguments of a stoichiometry.

We finally provide a generic formulation for $V_e(t)$ in (2). By putting together the notions of output flows (5), compartment mass flow dynamics (6), and additive flows (9), we can derive:

$$\frac{\mathrm{d}s_e(t)}{\mathrm{d}t} = -\sigma_e(t) - \sigma_e^{\eta}(t) + \tilde{\sigma}_e(t) + \sigma_e^{\iota}(t) \tag{10a}$$

$$\frac{\mathrm{d}\ell_e(t)}{\mathrm{d}t} = -\lambda_e(t) - \lambda_e^{\eta}(t) + \tilde{\lambda}_e(t) + \lambda_e^{\iota}(t) \tag{10b}$$

$$\frac{\mathrm{d}g_e(t)}{\mathrm{d}t} = -\gamma_e(t) - \gamma_e^{\eta}(t) + \tilde{\gamma}_e(t) + \gamma_e^{\iota}(t). \tag{10c}$$

Depending on the specific network element, some components of (10) can be null by definition. Take for simplicity the solid volume of network element e_1. If we assume no matter transformation takes place in e_1, which is a common assumption for storages, then $\sigma_{e_1}^{\eta}(t)$ and $\tilde{\sigma}_{e_1}(t)$ can be removed from the dynamical expression. Similarly, if e_1 does not distribute any matter to the rest of the network (e.g. a non-recyclable waste storage) or does not receive any matter from the rest of the network (e.g. a storage that is never refilled), then $\sigma_{e_1}(t)$ and $\sigma_{e_1}^{\iota}(t)$ can be respectively removed.

3. MELiSSA loop

As anticipated in Section 1, MELiSSA (Micro-Ecological Life Support System Alternative) is the leading project on advanced circular life support systems led by the European Space Agency, to support future crewed missions to deep space (MELiSSA Foundation). The driving element of MELiSSA is the recovery of food, water, oxygen, nitrogen and materials from organic waste, carbon dioxide, and minerals, using light as a source of energy to promote biological photosynthesis and with the objective of minimizing extra resources and buffers. It is inspired from a terrestrial lake ecosystem where waste products are processed using the metabolism of higher plants and micro-organisms, which in return provide food, air revitalization, and water purification. Thus, it represents a sustainable and environmentally friendly approach to life support systems for space missions, often referred to as functional ecology.

More in detail, the MELiSSA loop is a circular and regenerative LLS consisting of six interconnected compartments that serve different functions (Hendrickx and Mergeay, 2007). In the most up-to-date MELiSSA loop concept, shown in Fig. 3, c_1 is the thermophilic anaerobic compartment which starts the breakdown of waste from the rest of the loop; c_2 is a microbial electrolysis cell which further processes waste from c_1 converting them into useful byproducts; c_3 is the nitrifying compartment which recovers water and nutrient from crew urine for higher plants and microalgae; c_{4a} and c_{4b} are the microalgae and higher plants compartments which utilize nutrients, water and CO_2 produced in previous compartments to grow and produce oxygen, food and recover water thanks to plant transpiration; and c_5 is the crew compartment consuming resources and generating waste to feed c_1, thus closing the life support loop.

This compartmentalized structure is translated into a network structure (Fig. 4) to apply an engineering approach for the system development and to build a deterministic control strategy. The picture

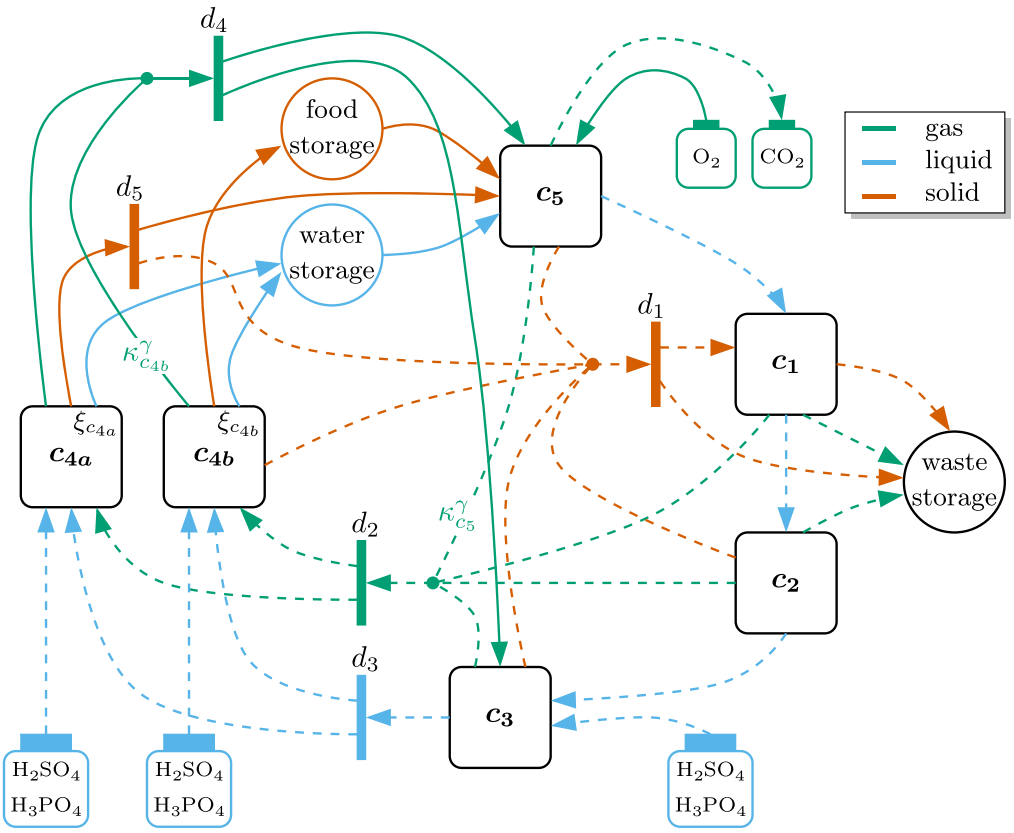

Fig. 4. Network structure for the MELiSSA loop highlighting the system compartments, storages, buffer tanks and their interconnections. Solid lines represent flows of resources for the crew, and dashed lines represent instead flows of waste. With colors we distinguish the different phases of the matter. Waste that cannot be recycled is represented by flows into the waste storage.

highlights the main elements of the loop and their exchanges in terms of gas, liquid, and solid flows. Each of the six compartments in this network should be represented by mechanistic models to apply a deterministic control strategy, but not all the models are currently at the same level of development (Vermeulen et al., 2023). Previous studies investigating advanced control approaches for the MELiSSA loop only focused on a portion of the network, for which advanced mechanistic models are available (Alemany et al., 2019; Ciurans et al., 2022). Since this work has the ambition of analyzing the *complete* MELiSSA loop, i.e., including all the compartments connected on all the phases (solid, liquid, and gas), a different approach must be followed. Hence, similarly to the work described in Thiron (2020) and Vermeulen et al. (2023), each compartment will be represented by one or more stoichiometric equations and a simple dynamical model.

The list of chemical components considered for each phase, which is the same for each network element (Thiron, 2020), is summarized in Table 1, along with their "CHONSP" compositions, i.e. their compositions in terms of Carbon (C), Hydrogen (H), Oxygen(O), Nitrogen (N), Phosphorus (P) and Sulfur (S). The stoichiometric equations that fully define $\upsilon_e(\cdot)$ in (6a) for each compartment are reported in the following sections.

3.1. Compartment c_1

There are four steps in the degradation occurring in c_1:

1. The urea flowing into c_1 is degraded according to Eq. (11a);
2. The organic matter flowing into c_1 is split in two parts: the matter to be degraded (*deg matter*) and the rest. Only a fixed percentage of the matter, set as a parameter, is degraded;
3. The composition of the matter to be degraded is fixed to $CH_{1.8}O_{0.5}N_{0.07}$ (Thiron, 2020). The composition of the rest of the organic matter, i.e. c_1 *waste*, is calculated in order to keep the CHONSP balance and it is sent directly to the waste storage;
4. The matter to be degraded is transformed as described in Eq. (11b).

$$CH_4ON_2 + H_2O \rightarrow CO_2 + 2\ NH_3 \tag{11a}$$

$$\begin{aligned} &deg\ matter + 0.1902\ H_2O \rightarrow 0.139\ C_2H_4O_2 \\ &+0.0159\ C_3H_6O_2 + 0.1114\ C_4H_8O_2 + 0.003\ C_6H_{12}O_2 \\ &+0.0488\ CO_2 + 0.0341\ H_2 + 0.07\ NH_3 + c_1\ waste \end{aligned} \tag{11b}$$

3.2. Compartment c_2

This compartment is responsible for the elimination of the terminal products of compartment c_1, according to the following equations:

$$\begin{aligned} &0.5\ C_2H_4O_2 + 0.852\ H_2O + 0.018\ NH_3 \\ &\rightarrow 0.1\ c_2\ biomass + 0.9\ CO_2 + 1.7915\ H_2 \end{aligned} \tag{12a}$$

$$\begin{aligned} &0.33\ C_3H_6O_2 + 1.185\ H_2O + 0.018\ NH_3 \\ &\rightarrow 0.1\ c_2\ biomass + 0.9\ CO_2 + 2.125\ H_2 \end{aligned} \tag{12b}$$

$$\begin{aligned} &0.25\ C_4H_8O_2 + 1.352\ H_2O + 0.018\ NH_3 \\ &\rightarrow 0.1\ c_2\ biomass + 0.9\ CO_2 + 2.2915\ H_2 \end{aligned} \tag{12c}$$

$$\begin{aligned} &0.167\ C_6H_{12}O_2 + 1.815\ H_2O + 0.018\ NH_3 \\ &\rightarrow 0.1\ c_2\ biomass + 0.9\ CO_2 + 2.458\ H_2 \end{aligned} \tag{12d}$$

Table 1
List of chemical components with their phase and composition. In "phase" column, "S" stands for Solids, "L" for liquids and "G" for gases.

Component	Phase	C	H	O	N	S	P
Proteins	S	1	1.5537	0.3104	0.2594	0.005	
Lipids	S	1	1.83	0.13			
Carbohydrates	S	1	1.75	0.9			
Nucleic acids	S	1	1.27	0.7	0.39		
EPS	S	1	1.65	0.95			
Fibers	S	1	1.65	0.82			
C1 biomass	S	1	1.64	0.52	0.16		
C2 biomass	S	1	1.75	0.52	0.18		
C3 biomass	S	1	1.6097	0.3777	0.2107	0.0041	0.0136
C4b NEP	S	1	1.43	0.62	0.017	0.007	
Water	L		2	1			
Urea	L	1	4	1	2		
Ammonia	L		3		1		
Nitrite	L		1	2	1		
Nitrate	L		1	3	1		
Sulfuric acid	L		2	4		1	
Phosphoric acid	L		3	4			1
Ethanol	L	2	6	1			
Acetate	L	2	4	2			
Propionate	L	3	6	2			
Butyrate	L	4	8	2			
Valerate	L	5	10	2			
Caproate	L	6	12	2			
Dioxygen	G & L			2			
Carbon dioxide	G & L	1		2			
Dinitrogen	G & L				2		
Dihydrogen	G & L		2				
Methane	G & L	1	4				

3.3. Compartment c_3

The nitrifying compartment's main function is to cycle ammonia evolved from waste to nitrates, which is the most favorable source of nitrogen for higher plants:

$$17.6726\ NH_3 + 25.1141\ O_2 + CO_2 + 0.0041\ H_2SO_4 + 0.00136\ H_3PO_4 \rightarrow 17.4619\ HNO_2 + 16.9976\ H_2O + c_3\ biomass \quad (13a)$$

$$0.2107\ NH_3 + 36.8247\ HNO_2 + 17.3337\ O_2 + CO_2 + 0.0041\ H_2SO_4 + 0.00136\ H_3PO_4 + 0.4643\ H_2O \rightarrow 36.8247\ HNO_3 + c_3\ biomass \quad (13b)$$

3.4. Compartment c_{4a}

Two equations are considered in this compartment for the oxygen and spirulina production. Stoichiometric coefficients are not fixed and are recalculated at each iteration according to the spirulina composition, which is as well recalculated at each iteration as a function of the light intensity:

$$CO_2 + a\ HNO_3 + b\ H_2SO_4 + c\ H_3PO_4 \rightarrow d\ spirulina + e\ O_2 + f\ H_2O \quad (14a)$$

$$CO_2 + a\ NH_3 + b\ H_2SO_4 + c\ H_3PO_4 \rightarrow d\ spirulina + e\ O_2 + f\ H_2O \quad (14b)$$

3.5. Compartment c_{4b}

Two equations are considered in this compartment for oxygen production and plant growth. Stoichiometric coefficients are not fixed and are calculated according to the composition of the edible part and non edible part of the plants, respectively EP and NEP:

$$CO_2 + a\ HNO_3 + b\ H_2SO_4 + c\ H_2O \rightarrow d\ EP + e\ NEP + f\ O_2 \quad (15a)$$

$$CO_2 + a\ NH_3 + b\ H_2SO_4 + c\ H_2O \rightarrow d\ EP + e\ NEP + f\ O_2 \quad (15b)$$

3.6. Compartment c_5

The stoichiometric coefficients of the crew compartment equation are not fixed and are recalculated at each iteration according to the composition of the input food:

$$a\ food + b\ O_2 \rightarrow c\ CO_2 + d\ CH_4ON_2 + e\ faeces + f\ H_2O + g\ H_2SO_4 + h\ H_3PO_4 + i\ NH_3 + l\ H_2 + m\ CH_4 \quad (16a)$$

4. Regenerative LSS network architecture

We make use of the building blocks introduced in Section 2 to derive the global model (1) of one of the regenerative LSS network architectures analyzed in the MELiSSA project, which is depicted in Fig. 4. From now on, we will address as *elements* only the architectural items of Fig. 4 that, for the specific formulation here presented, require explicit model states, and which are $\mathcal{E} = \{c_1, c_2, c_3, c_{4a}, c_{4b}, c_5, q, h\}$ with c_1 the thermophilic anaerobic bioreactor, c_2 the microbial electrolysis cell, c_3 the nitrifying bioreactor, c_{4a} the microalgae photobioreactor, c_{4b} the higher plants compartment, c_5 the crew, q and h representing the *food* and *water storage*, respectively. The *waste storage* gathers all the waste that the system cannot recycle, but it does not need to be explicitly modeled as a network element because the controller tasks can be tackled by the sole regulation of the flows that would contribute to its filling. The list of chemical components considered for each phase is summarized in Table 1, and they are the same for each network element (Thiron, 2020). It follows that $n_s = 10$, $n_\ell = 18$ and $n_g = 5$, $\forall e \in \mathcal{E}$. We define $m_s \in \mathbb{R}^{n_s}_{>0}$, $m_\ell \in \mathbb{R}^{n_\ell}_{>0}$ and $m_g \in \mathbb{R}^{n_g}_{>0}$ the molar masses (g/mol) of the corresponding solid, liquid, and gas components. We instead refer to $m_{[\chi]}$ as the molar mass of χ. Lastly, let us define $l_{\text{food}} \in \mathbb{R}^6_{\geq 0}$ as the list of the first six solid elements in Table 1, and representing the array of "food", namely the edible components of the solid phase.

4.1. Modeling ingredients

We first introduce the time-varying vector $\theta(t)$ model parameters because the definition of some flow connections will depend on them:

$$\theta(t) = \begin{bmatrix} \bar{f}(t) \\ \mathcal{D}(t) \\ \langle H_2O \rangle_{c.}(t) \\ \langle O_2 \rangle_{c.}(t) \\ \langle CO_2 \rangle_{p.}(t) \end{bmatrix} \tag{17}$$

where:

- $\bar{f}(t) \in \mathbb{R}_{>0}$ is the flow (g/d) of dry mass of food needed by the crew,
- $\mathcal{D}(t) \in \mathbb{R}^6_{\geq 0}$ is the prescribed optimal diet for the crew, expressed as

$$\mathcal{D}(t) = \begin{bmatrix} \mathcal{D}_{\text{proteins}}(t) \\ \mathcal{D}_{\text{lipids}}(t) \\ \mathcal{D}_{\text{carbohydrates}}(t) \\ \mathcal{D}_{\text{nucleic}}(t) \\ \mathcal{D}_{\text{eps}}(t) \\ \mathcal{D}_{\text{fibers}}(t) \end{bmatrix} \tag{18}$$

  where $\mathcal{D}_\chi(t)$ represents the normalized ratio of the solid component χ in the diet of the crew, and such that $\|\mathcal{D}(t)\|_1 = 1$,
- $\langle H_2O \rangle_{c.}(t)$ represents the flow (g/d) of drinkable water needed by the crew,
- $\langle O_2 \rangle_{c.}(t)$ the flow (g/d) of oxygen needed by the crew in the cabin,
- $\langle CO_2 \rangle_{p.}(t)$ the flow (g/d) of CO_2 needed by the higher plants that are being cultivated in c_{4b} compartment.

The parameters are time-varying to allow the simulation of different crew activities, diets, and biomass growth.

In the network, there are five distributors, which translates into the manipulated variables d_j, with $j = 1, \dots, 5$, whose input flows are designed according to Fig. 2 as in the following equations (we have dropped the dependence from t for simplicity):

$$\delta_1 = \sigma_{c_2} + \sigma_{c_3} + (\sigma_{c_{4a}} - \bar{f}_s \circ \frac{1}{24 m_s}) + \text{NEP}(\sigma_{c_{4b}}) + \sigma_{c_5} \tag{19a}$$

$$\delta_2 = \gamma_{c_1}|_{H_2=0} + \gamma_{c_2}|_{H_2=0} + \lambda^g_{c_{4a}} + \lambda^g_{c_{4b}} + \gamma_{c_3} + \gamma_{c_5} \tag{19b}$$

$$\delta_3 = \lambda_{c_3} \tag{19c}$$

$$\delta_4 = \gamma_{c_{4a}} + \gamma_{c_{4b}} \tag{19d}$$

$$\delta_5 = \sigma_{c_{4a}} \tag{19e}$$

where "$\circ$" indicates the Hadamard product, NEP stands for the non-edible plant parts according to Table 1, $\bar{f}_s(t)$ is the flow (g/d) of spirulina, in solid phase, that is being eaten by the crew. Clearly, $\bar{f}_s \circ (1/(24 m_s)) = d_5(t)\sigma_{4a}(t)$ holds true, and $\bar{f}_{s,[\chi]}(t) = 0$, $\forall \chi \notin l_{\text{food}}$, $\forall t > t_0$, being t_0 the initial time.

Remark 4.1. The quantity $\sigma_{c_{4a}}(t)$ corresponds to the flow of spirulina biomass grown in the microalgae photobioreactor, but there exist safety limits to its consumption by the crew, explained in the requirements section, and therefore it is compulsory to introduce $\bar{f}_s$. Distributor d_1 splits the non-edible solids produced by the different compartments between c_1 and the waste storage. Air that is rich in CO_2 and the liquids produced by the nitrification stage are split between the microalgae photobioreactor and higher plant compartments by means of d_2 and d_3, respectively. The term d_4 hands out air that is rich in O_2, and therefore collected from c_{4a} and c_{4b}, to c_5 (the crew) and c_3. The term d_5 supplies the crew with the needed spirulina biomass and routes the rest to d_1.

4.2. Complete dynamics of the selected architecture

The model in (6) generalizes the output flow-model of the compartments. Table 2 collects the time-constants for each phase and compartment combination. Each output flow-model is then uniquely defined in terms of the input flows $\sigma^l_e(t)$, $\lambda^l_e(t)$, $\gamma^l_e(t)$. For each element, they are determined by a nonlinear function of manipulated variables and output flows of other network elements, which we derive later on. We start by exposing some features of the examined network:

- $\xi_{4a}(t)$, $\xi_{4b}(t) \in [0, 100]$ are the only *activities* that are being considered, and they can be interpreted as an actuator on the average light intensity for c_{4a} and c_{4b};
- besides food and water storage, volumes are modeled only in c_{4b} and c_5 and, more in detail, we model $g_{c_{4b}}(t)$ and $g_{c_5}(t)$ which represent volumes of the gases in the atmospheres of the greenhouse and the cabin, respectively;
- as a consequence of the previous point, $\kappa^\gamma_{c_{4b}}(t)$ and $\kappa^\gamma_{c_5}(t)$ are the flows that can be manipulated by the controller.

Let $\mu^\gamma_{c_{4b}}(t)$, $\mu^\gamma_{c_5}(t) \in \mathbb{R}_{\geq 0}$ be the gas flows induced by the higher plants and the crew, respectively, such that

$$\mu^\gamma_{c_{4b}}(t) = \frac{\langle CO_2 \rangle_{p.}(t)}{24 m_{[CO_2]} g_{c_{4b},[CO_2]}(t)} \tag{20a}$$

$$\mu^\gamma_{c_5}(t) = \frac{\langle O_2 \rangle_{c.}(t)}{24 m_{[O_2]} g_{c_5,[O_2]}(t)} \tag{20b}$$

then the quantities $\mu^\gamma_{c_{4b}}(t)\pi(g_{c_{4b}}(t))$ and $\mu^\gamma_{c_5}(t)\pi(g_{c_5}(t))$ can be interpreted respectively as the respiration activity (mol/h) of the higher plants and the crew. It corresponds to the amount of gas components that are ingested, given the current composition of air, to satisfy the needs of CO_2 for the higher plants and O_2 for the crew according to (17). Similarly, let $\mu^\lambda_{c_{4b}}(t)$ be the liquid flow induced by the crew, such that:

$$\mu^\lambda_{c_5}(t) = \frac{\langle H_2O \rangle_{c.}(t)}{24 m_{[H_2O]} \ell_{h,[H_2O]}(t)} \tag{21}$$

then $\mu^\lambda_{c_5}(t)\pi(\ell_h(t))$ represent the drinking activity (mol/h) of the crew.

Let $\bar{f}_q(t)$ be the flow (g/d) of food components that the crew takes out from the food storage. Given (17), we have that:

$$\bar{f}_q(t) = \mathcal{D}(t)\bar{f}(t) - \bar{f}_s(t) \tag{22}$$

where we recall that $\bar{f}_s(t)$ is the flow of spirulina eaten. Clearly, $\|\bar{f}_q(t) + \bar{f}_s(t)\|_1 = \bar{f}(t)$ holds true, meaning that the requirement regarding the amount of dry food mass eaten by the crew is satisfied. From (18) and (22) it follows that $\bar{f}_{q,[\chi]}(t) = 0$, $\forall \chi \notin l_{\text{food}}$, $\forall t > t_0$.

With the assumptions on the network structure listed above, and considering the modeling tools introduced in Sections 2 and 4.1, the compartments input flows can be expressed as follows:

$$\Phi^l_{c_1}(t) = \begin{bmatrix} \delta_1(t) d_1(t) \\ \lambda^\ell_{c_{4a}}|_{H_2O=0}(t) + \lambda^\ell_{c_{4b}}|_{H_2O=0}(t) + \lambda_{c_5}(t) \\ \mathbf{0}_{n_g} \end{bmatrix} \tag{23a}$$

$$\Phi^l_{c_2}(t) = \begin{bmatrix} \mathbf{0}_{n_s} \\ \lambda_{c_1}(t) \\ \mathbf{0}_{n_g} \end{bmatrix} \tag{23b}$$

$$\Phi^l_{c_3}(t) = \begin{bmatrix} \mathbf{0}_{n_s} \\ \lambda_{c_2}(t) + \lambda_{\overrightarrow{c_3}}(t) \\ \delta_4(t) d_4(t) \end{bmatrix} \tag{23c}$$

$$\Phi^l_{c_{4a}}(t) = \begin{bmatrix} \mathbf{0}_{n_s} \\ \delta_3(t) d_3(t) + \lambda_{\overrightarrow{c_{4a}}}(t) \\ \delta_2(t) d_2(t) + \gamma_{\overrightarrow{c_{4a}}}(t) \end{bmatrix} \tag{23d}$$

Table 2
Time constants for the different compartments.

Compartment	τ^s	τ^{ℓ}	τ^g
c_1	160 h	8 h	1 h
c_2	160 h	8 h	1 h
c_3	30 h	3 h	0.1 h
c_{4a}	120 h	8 h	0.2 h
c_{4b}	120 h	8 h	0.2 h
c_5	8 h	1 h	0.1 h

$$\boldsymbol{\Phi}^{I}_{c_{4b}}(t) = \begin{bmatrix} \mathbf{0}_{n_s} \\ \delta_3(t)(1-d_3(t)) + \lambda_{\overline{c_{4b}}}(t) \\ \mu^{\gamma}_{c_{4b}}(t)\pi(g_{c_{4b}}(t)) \end{bmatrix} \tag{23e}$$

$$\boldsymbol{\Phi}^{I}_{c_5}(t) = \begin{bmatrix} (\bar{f}_q(t) + \bar{f}_s(t)) \circ \frac{1}{24 m_s} \\ \mu^{\lambda}_{c_5}(t)\pi(\ell_h(t)) \\ \mu^{\gamma}_{c_5}(t)\pi(g_{c_5}(t)) \end{bmatrix}. \tag{23f}$$

As far as volumes are considered, the atmosphere in the c_{4b} greenhouse and in the cabin, the food, and water storages are respectively modeled as:

$$\frac{\mathrm{d}g_{4b}(t)}{\mathrm{d}t} = \delta_2(t)(1-d_2(t)) + \tilde{\gamma}_{c_{4b}}(t) - \kappa^{\gamma}_{c_{4b}}(t)\pi(g_{c_{4b}}(t)) - \mu^{\gamma}_{c_{4b}}(t)\pi(g_{c_{4b}}(t)) + \gamma_{\overline{c_{4b}}}(t) \tag{24a}$$

$$\frac{\mathrm{d}g_{c_5}(t)}{\mathrm{d}t} = \delta_4(t)d_4(t) + \tilde{\gamma}_{c_5}(t) - \kappa^{\gamma}_{c_5}(t)\pi(g_{c_5}(t)) - \mu^{\gamma}_{c_5}(t)\pi(g_{c_5}(t)) + \gamma_{\overline{c_5}}(t) \tag{24b}$$

$$\frac{\mathrm{d}s_q(t)}{\mathrm{d}t} = \sigma_{c_{4b}}|_{\mathrm{NEP}=0}(t) - \bar{f}_q(t) \circ \frac{1}{24 m_s} \tag{24c}$$

$$\frac{\mathrm{d}\ell_h(t)}{\mathrm{d}t} = \mathrm{H_2O}(\lambda_{c_{4a}}(t)) + \mathrm{H_2O}(\lambda_{c_{4b}}(t)) - \mu^{\lambda}_{c_5}(t)\pi(\ell_h(t)). \tag{24d}$$

This is a realization of the generic formulation (10). From (24c) we get that the food tank is filled up by just c_{4b}, whereas the water tank receives drinkable water from both c_{4a} and c_{4b}. This follows from the fact that in this work we assume that spirulina (i.e., the part of food produced in c_{4a}) cannot be preserved for a long time. Thus, $\sigma_{4a}(t)$ does not pass through an intermediate state of a food storage system. The requirements for the regenerative LSS include the production of only a part of the food and water needs of the crew (the exact values adopted in this paper for the sake of demonstration are detailed in Section 5). Then it is evident that $s_{q,[\chi]}(0) > 0,\ \forall \chi \in l_{\text{food}}$ and $s_{q,[\chi]}(0) = 0, \forall \chi \notin l_{\text{food}}$. Similarly, we have that $\ell_{h,[\chi]}(0) = 0,\ \forall \chi \neq \mathrm{H_2O}$ and $\ell_{h,[\mathrm{H_2O}]}(0) > 0$. Additionally, from (22), (24c) and (24d) it follows that $s_{q,[\chi]}(t) = 0, \forall \chi \notin l_{\text{food}}, \forall t \geq t_0$ and $\ell_{h,[\chi]}(t) = 0, \forall \chi \neq \mathrm{H_2O}, \forall t \geq t_0$, which means that the food and water tank contain only just food and water at any point in time, respectively.

Remark 4.2. The complete flow model of the MELiSSA loop is mathematically described by the combination of the input flows and volumes equations. For the architecture described here, they are respectively collected in Eqs. (23) and (24).

5. Model predictive control formulation

Regenerative LSS are systems with complex dynamics, which require the coordination of many compartments and storage systems in a circular network. The processes involved are very different in nature, for instance, biological, chemical, and thermodynamic, and so are their timescales. Control requirements are also heterogeneous and mostly conflicting. Considering the limits of the available model formulation for the MELiSSA compartments, in this work we took into account the following criteria: circularity, survival, energy efficiency and use of resources. Such requirements are based upon the ALiSSE (Advanced Life Support System Evaluator) criteria used for evaluation and trade-off of any life support system (Brunet et al., 2010). A definition of each of these criteria, formulated in the form of cost functions to minimize or constraints to satisfy, is given in the following sections. Furthermore, many activities that concern the crew can be easily predicted as they follow a well-defined schedule that is possibly adapted in real-time by the mission planner. This preview of control requirements in a future time window can be very effectively exploited by an MPC algorithm to improve performances. For the R&D feasibility studies that have to be currently conducted in the MELiSSA framework, the modularity and ease of upgrade is a further driving factor for the selection of the supervisory strategy. All the aforementioned characteristics make MPC the preferred choice for the global coordination of the MELiSSA network. MPC explicitly uses the model of the system to predict its dynamic evolution over p steps in the future and computes the control action by iteratively solving a finite-time constrained optimal control problem, repeating the optimization process at each time step after shifting the prediction window forward. The resulting "receding horizon" operation of MPC is depicted in Fig. 5.

5.1. Formulation of the nonlinear MPC controller

We briefly describe the formulation of the MPC controller that we use in this work. That is the one adopted in the *ODYS Embedded MPC* software (ODYS, 2019; Cimini et al., 2017), which we employed to implement and test the controller. Let the system dynamics be described by (1). We sample the prediction window $[t, t+t_h]$ in a sequence of discrete time instants $[t+T(0), t+T(1), \dots, t+T(p)]$, with p the prediction steps and $T(0) = 0$, $T(p) = t_h$. The nonlinear model is simulated in prediction from $x(t)$ up to $x(t+t_h)$. Given the current state $x(t)$ and a nominal input sequence $\bar{u}(t)$, a Linear Time-Varying (LTV) model, Falcone et al. (2008), that approximates (1) can be obtained by computing the corresponding nominal state sequence $\bar{x}(t)$ and the associated sensitivity matrices according to the following procedure:

1. let $\bar{x}(t) \equiv x(t)$
2. for $k = 0, \dots, p-1$ do:
   - (2.1) get $\bar{u}(t+T(k))$ from nominal input and parameter sequences
   - (2.2) get $\bar{x}(t+T(k+1))$ by numerically integrating the non-linear model between $t+T(k)$ and $t+T(k+1)$
   - (2.3) get the sensitivities

$$A(t+T(k)) = \frac{\partial \bar{x}(t+T(k+1))}{\partial \bar{x}(t+T(k))} \tag{25a}$$

$$B(t+T(k)) = \frac{\partial \bar{x}(t+T(k+1))}{\partial \bar{u}(t+T(k))} \tag{25b}$$

Then, we have that

$$x(k+1) = \bar{x}(k+1) + A(k)(x(k) - \bar{x}(k)) + B(k)(u(k) - \bar{u}(k)) \tag{26}$$

is an LTV approximation of (1), where the shortened notation $x(k) \triangleq x(t+T(k))$ will be used for the rest of the paper. A quadratic optimization problem (QP) based on model (26) is iteratively built and solved, leading to a form of Sequential Quadratic Programming (SQP); see ODYS (2019) for a detailed description.

Before designing the cost and constraints of the optimal control problems, the set of manipulated variables should be identified. The network has five distributors, see (19), however an optimal split of spirulina can be analytically derived. Let $D^{\max}_{\text{spiru}}$ be the maximum normalized ratio of spirulina that the crew can eat daily. Under the assumption that $\sigma_{4a}(t)$ is just spirulina and that once produced, if not exceeding toxicity bounds, there is no reason for the crew not to eat it, then the optimal value for $d_5(t)$ is:

$$d_5(t) = \min\left(1, \frac{D^{\max}_{\text{spiru}} \bar{f}(t)}{\|\sigma_{c_{4a}}(t) \circ m_s\|_1}\right). \tag{27}$$

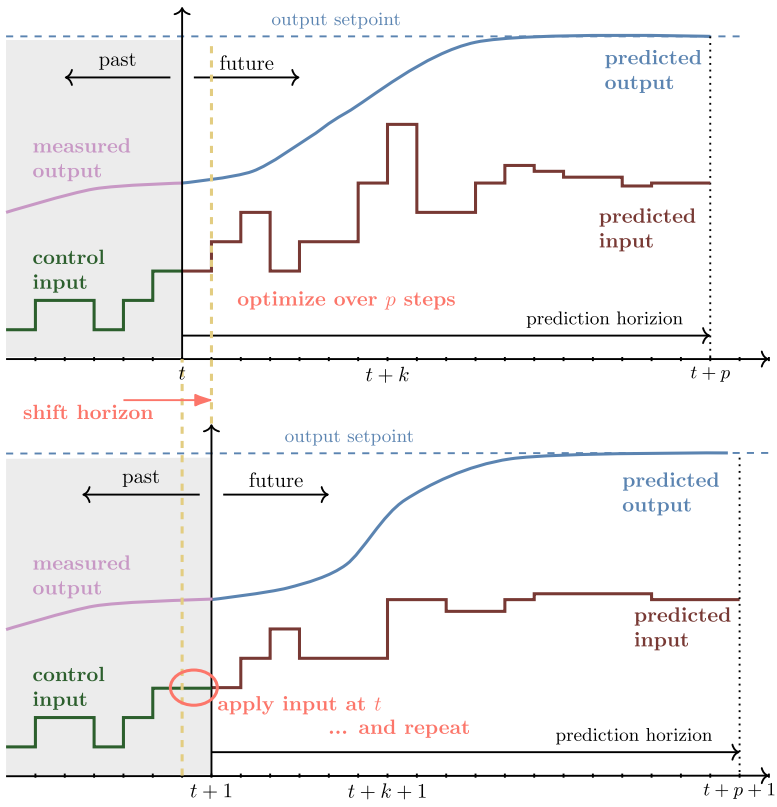

Fig. 5. Receding horizon operation for an MPC controller evaluated at time t with p prediction steps. The optimal control sequence is computed (top figure), and then only the first move is applied at $t+1$ (bottom figure).

Several studies have addressed the positive and negative aspects of spirulina as a food complement in astronaut diets as reviewed in Fahrion et al. (2021). Here, we set $\mathcal{D}^{\max}_{\text{spiru}} = 0.05$, which amounts to a maximum of 5% of spirulina in the crew diet. We stress that:

$$\frac{\bar{f}_q(t) + \bar{f}_s(t)}{\|\bar{f}_q(t) + \bar{f}_s(t)\|_1} = \mathcal{D}(t). \tag{28}$$

Remark 5.1. One of the control requirements is to satisfy crew's and higher plants' needs in terms of solid, liquid, and gas flows, according to the parameter vector $\theta(t)$ in (17). However, here, we assume not to have any authority in altering the eating, drinking, and respiration behavior of crew and higher plants so that if $\theta(t)$ cannot be satisfied at any point in time, the simulation is considered failed. This is why $\theta(t)$ directly drives the behavior of some of the flows in the network without the need for specific manipulated variables.

From the previous considerations and the network elements' models introduced in Sections 4.1 and 4.2 we can formalize the set of variables $u(t) \in \mathbb{R}^{n_u}$ being manipulated by the MPC supervisor:

$$u(t) = \begin{bmatrix} d_1(t) & d_2(t) & d_3(t) & d_4(t) & \xi_{c_{4a}}(t) & \xi_{c_{4a}}(t) \\ \kappa^{\gamma}_{c_{4b}}(t) & \kappa^{\gamma}_{c_5}(t) & \rho(t)^{\intercal} \end{bmatrix}^{\intercal} \tag{29}$$

where we indicate by $\rho(t) \in \mathbb{R}^{n_\rho}$ the set of flows from/to the buffer tanks, whose selection represents what here is addressed as *network architecture*. In Section 6, we will show results obtained with different architectures. For instance if all the additional components depicted in Fig. 4 were considered, then we would have $n_\rho = 8$ and $n_u = 16$, with:

$$\rho = \begin{bmatrix} \langle H_3PO_4\rangle_{\overrightarrow{c_3}} & \langle H_2SO_4\rangle_{\overrightarrow{c_3}} & \langle H_3PO_4\rangle_{\overrightarrow{c_{4a}}} & \langle H_2SO_4\rangle_{\overrightarrow{c_{4a}}} \\ \langle H_3PO_4\rangle_{\overrightarrow{c_{4b}}} & \langle H_2SO_4\rangle_{\overrightarrow{c_{4b}}} & \langle O_2\rangle_{\overrightarrow{c_5}} & \langle CO_2\rangle_{\overrightarrow{c_5}} \end{bmatrix}^{\intercal}. \tag{30}$$

Moreover, we impose $\rho_j \geq 0$, $j = 1, \dots, 7$, meaning that all the additional components can be just added to the system, besides $\rho_8 = \langle CO_2\rangle_{\overrightarrow{c_5}}$ which instead can also be negative, allowing for the existence of a CO_2 extractor device in the cabin crew. The set of flows from/to the buffer tanks in (30) is the worst-case that has been considered during the architectures' investigation.

In the following sections, we design the different components of the cost function and constraints for the MPC controller according to the system requirements.

5.2. Recycling and recovery

One of the main objectives of MELiSSA is the production of metabolic resources based on waste valorization. The MELiSSA loop is a circular system where part of the organic wastes can be degraded by c_1 to recover as much usable matter as possible. CO_2, NH_3, and volatile fatty acids can indeed be produced by chemical and biological transformations. The model of c_1 acts at present as a pass-through, without any direct actuation that can modify its behavior, and therefore, waste minimization is achievable only by optimally manipulating flows that maximize c_1 activity. Moreover, we assume that the matter extracted by means of a manipulated sink cannot be reused by the system and, therefore, contributes to an increase in waste. A direct minimization of the production of waste in the cost function is a proxy to maximize the circularity of the LSS. For the control-oriented model, the dynamics characterization of waste storages is unnecessary as waste production can be minimized by penalizing specific output flows. Let $\omega_\sigma(t) \in \mathbb{R}^{n_s}_{\geq 0}$ and $\omega_\gamma(t) \in \mathbb{R}^{n_g}_{\geq 0}$ be set of weights penalizing solid and gas waste, respectively. Let $\omega_{CO_2}(t) \in \mathbb{R}_{\geq 0}$ penalize the use of CO_2 direct air capture system. Then $W_1(t) \in \mathbb{R}_{\geq 0}$ denotes the recycling and recovery contribution to the cost, expressed as a function of the grams of waste produced, and defined as:

$$W_1(t) = \left(m_s \circ \omega_\sigma(t)\right)^{\intercal} \left(\delta_1(t)(1 - d_1(t))\right) + \left(m_g \circ \omega_\gamma(t)\right)^{\intercal} \left(H_2(\gamma_{c_1}(t)) + H_2(\gamma_{c_2}(t))\right)$$

$$+ m_{[CO_2]}\omega_{CO_2}(t)\max(0, -\langle CO_2\rangle_{\overline{c_5}}(t)) \tag{31}$$

where the first term of $W_1(t)$ penalizes the waste handed out by $d_1(t)$, the second term penalizes the gas waste produced by c_1 and c_2, and the last penalizes the CO_2 removed from the cabin, for which, in this work, we assume that it cannot be reinserted in the loop.

Remark 5.2. Proper values for the weights can be set by taking into account the cost to store a specific chemical component in its waste form and how useful a chemical component is during the course of the mission and after its completion. Therefore, they could be very different from one chemical component to the other and also time-varying. In this work we assume that $\omega_{\sigma,i}(t) = \omega_{\gamma,j}(t)$, $\forall i \in \{1,\dots,n_s\}$, $\forall j \in \{1,\dots,n_g\}$, $\forall t > t_0$.

5.3. Use of extra resources

The ultimate goal for a regenerative LSS is to operate without the need of any extra resource that can be provided by buffer tanks. During this research stage, buffer tanks, manipulated by the controller, exist to investigate different architectures. A dense use of multiple chemical components at different injection points can be planned in order to design an optimal architecture that simultaneously minimizes the mass of extra tanks to carry on board while maximizing the circularity. Regarding the real-time MPC controller, we include a term in the cost function, namely $W_2(t) \in \mathbb{R}_{\geq 0}$, that penalizes the use of buffer tanks. Let $\omega_{\sigma_{\overrightarrow{e}}} \in \mathbb{R}^{n_s}_{\geq 0}(t)$, $\omega_{\lambda_{\overrightarrow{e}}} \in \mathbb{R}^{n_\ell}_{\geq 0}(t)$ and $\omega_{\gamma_{\overrightarrow{e}}} \in \mathbb{R}^{n_g}_{\geq 0}(t)$ be the weights for solid, liquid, and gas additional chemical components at the inlet of eth compartment, then according to (23) it follows that:

$$W_2(t) = \sum_{e\in\{c_3,c_{4a},c_{4b}\}} \left(m_\ell \circ \omega_{\lambda_{\overrightarrow{e}}}(t)\right)^\intercal \max(0, \lambda_{\overrightarrow{e}}(t)) + \sum_{e\in\{c_{4a},c_{4b},c_5\}} \left(m_g \circ \omega_{\gamma_{\overrightarrow{e}}}(t)\right)^\intercal \max(0, \gamma_{\overrightarrow{e}}(t)). \tag{32}$$

Remark 5.3. Weights for buffer tanks can be set by considering the type of chemical component, the injection point, and the hardware necessary to store it for a long time. The cost of using a specific chemical component may also increase/decrease over the course of a mission, depending on its scarcity. In this work, we assume that $\omega_{\lambda_{\overrightarrow{e_1}},i}(t) = \omega_{\gamma_{\overrightarrow{e_2}},j}(t)$, $\forall i \in \{1,\dots,n_\ell\}$, $\forall j \in \{1,\dots,n_g\}$, $\forall e_1 \in \{c_3, c_{4a}, c_{4b}\}$, $\forall e_2 \in \{c_{4a}, c_{4b}, c_5\}$, $\forall t > t_0$.

5.4. Energy efficiency

Stoichiometric models of compartments and the flows' connections at the network level do not model energy phenomena as per in Section 2. Energy efficiency is, however, a crucial control performance metric and can be already addressed, at least partially, by penalizing those manipulated variables that have an impact on it. Specifically, from $u(t)$ definition in (29), lights and recirculation of manipulated flows can be included into an energy-related cost term $W_3(t) \in \mathbb{R}_{\geq 0}$, as:

$$W_3(t) = \omega_{\underline{\xi}_{c_{4a}}}(t)\underline{\xi}_{c_{4a}}(t) + \omega_{\underline{\xi}_{c_{4b}}}(t)\underline{\xi}_{c_{4b}}(t) + \omega_{\underline{\kappa}^\gamma_{c_{4b}}}(t)\underline{\kappa}^\gamma_{c_{4b}}(t) + \omega_{\underline{\kappa}^\gamma_{c_5}}(t)\underline{\kappa}^\gamma_{c_5}(t) \tag{33}$$

where $\omega_{\underline{\xi}_{c_{4a}}}(t)$, $\omega_{\underline{\xi}_{c_{4b}}}(t)$, $\omega_{\underline{\kappa}^\gamma_{c_{4b}}}(t)$, $\omega_{\underline{\kappa}^\gamma_{c_5}}(t) \in \mathbb{R}_{\geq 0}$, are the weights.

5.5. Actuator bounds

All actuators can take values in a certain range, which usually is dictated by hardware limitations. Such limitations are imposed as inequality constraints on the optimization variables $u(t)$. Given a generic $z \in \mathbb{R}^n$, let $\underline{z} \in \mathbb{R}^n$ and $\bar{z} \in \mathbb{R}^n$ denote, respectively, the lower and upper bounds on z. Typically distributors take values in the range $[0, 1]$, however here we set $\underline{d}_j(t) \leq d_j(t) \leq \bar{d}_j(t)$, with $\underline{d}_j(t), \bar{d}_j(t) \in \mathbb{R}_{\geq 0}$ and $\underline{d}_j(t) + \bar{d}_j(t) = 1$, $j = 1,\dots,4$. It is, therefore, possible to instruct MPC to always guarantee a minimum input flow for a specific compartment. Light intensities are such that $\underline{\xi}_e(t) \leq \xi_e(t) \leq 100$, $e \in \{c_{4a}, c_{4b}\}$, with a non-zero lower bound in order to guarantee a minimum transformation rate for the compartments' stoichiometry. Manipulated flows are constrained such that $0 \leq \underline{\kappa}^\gamma_{c_{4b}}(t) \leq \bar{\kappa}^\gamma_{c_{4b}}(t)$, $0 \leq \underline{\kappa}^\gamma_{c_5}(t) \leq \bar{\kappa}^\gamma_{c_5}(t)$, which allow MPC to not circulate gas from atmospheres at a given point in time. Similarly, the flows of buffer tanks are such that $\langle\underline{\chi}\rangle_e(t) \leq \langle\chi\rangle_e(t) \leq \langle\bar{\chi}\rangle_e(t), \forall\langle\bar{\chi}\rangle_e \in u$, where $\langle\underline{\chi}\rangle_e(t) = 0$ and $\langle\bar{\chi}\rangle_e(t) = 0$ mean that there is no sink or additive capability, respectively.

5.6. Storage constraints

Storages and compartments' volumes are obviously non-negative and have specific maximum capacities. We therefore limit the total volume of cabin and greenhouse atmospheres, as well as food and water tank:

$$0 \leq \|g_{c_{4b}}(t)\|_1 \leq \bar{g}_{c_{4b}}(t) \tag{34a}$$

$$0 \leq \|g_{c_5}(t)\|_1 \leq \bar{g}_{c_5}(t) \tag{34b}$$

$$0 \leq \|s_q(t)\|_1 \leq \bar{s}_q(t) \tag{34c}$$

$$0 \leq \|\ell_h(t)\|_1 \leq \bar{\ell}_h(t). \tag{34d}$$

Considering that crew and higher plants needs are model parameters (i.e. the dynamics directly depend on their value), and to make the controller robust against possible faults, it is compulsory to impose positive lower bounds on specific components of volumes. That is the case for the quantities that dictate respiration activities in (20a). To this end, we impose:

$$g_{c_{4b},[CO_2]}(t) \geq 6\langle CO_2\rangle_{\text{p.}}(t) \tag{35a}$$

$$g_{c_5,[O_2]}(t) \geq 6\langle O_2\rangle_{\text{c.}}(t) \tag{35b}$$

that satisfies the requirement that the MELiSSA loop should provide 100% of the crew oxygen needs at any point in time, and with a safety margin of 6 h in case the cabin or the greenhouse is isolated and no buffer tank can be used.

5.7. Safety and survivability constraints

Besides the one already covered by previous sections, a series of requirements concern the system's safety and the crew's survivability. For safety reasons (flammability), the O_2 partial pressure in the greenhouse should not be greater than 24%, which can be imposed as:

$$\frac{g_{c_{4b},[O_2]}(t)}{\|g_{c_{4b}}(t)\|_1} \leq 0.24. \tag{36}$$

Similarly, for safety reasons (flammability) and for the survivability of the crew, the O_2 partial pressure in the cabin should be between 19% and 23%:

$$0.19 \leq \frac{g_{c_5,[O_2]}(t)}{\|g_{c_5}(t)\|_1} \leq 0.23. \tag{37}$$

For the crew survival, the CO_2 concentration in the cabin should be lower than 5000 ppm:

$$\frac{g_{c_5,[CO_2]}(t)}{\|g_{c_5}(t)\|_1} \leq 0.005. \tag{38}$$

In this paper we assume that the MELiSSA loop should produce at least 40% of the food crew's needs. As a ratio, it can be directly imposed on solid flows. Under the assumptions that solid flow from c_{4a} is spirulina and that solid flow from c_{4b} is food if NEP is removed, then:

$$\|\sigma_{c_{4a}}(t) + \sigma_{c_{4b}}|_{\text{NEP}=0}(t)\|_1 \geq 0.4\frac{\bar{f}(t)}{24m_s}. \tag{39}$$

We recall that the safe daily amount of spirulina is guaranteed by the optimal selection of $d_5(t)$, see (27). The MELiSSA loop should also

produce, at least, 90% of the drinkable water that is needed by the crew ($\langle H_2O\rangle_{c.}$). Such constraint can be directly imposed on the liquid output flows of c_{4a} and c_{4b}:

$$\|\lambda_{c_{4a},[H_2O]}(t) + \lambda_{c_{4b},[H_2O]}(t)\|_1 \geq 0.9\langle H_2O\rangle_{c.}(t). \tag{40}$$

Lastly, higher plants and microalgae should not receive a toxic amount of ammonia, which could be enforced with a constraint on c_3 output flow:

$$\frac{\lambda_{c_3,[NH_3]}(t)}{\lambda_{c_3,[HNO_3]}(t)} \leq 0.2. \tag{41}$$

5.8. Finite-time optimal control problem

While Sections from 5.2 to 5.7 describe elements of the optimal control problem that are directly linked to MELiSSA requirements, we have equipped the MPC formulation with few additional expedients to improve control performance. Consider the constraints in (34): given (39) and (40), it follows that $\|s_q(t_1)\|_1 > \|s_q(t_2)\|_1$ and $\|\ell_h(t_1)\|_1 > \|\ell_h(t_2)\|_1$, if $t_1 \gg t_2$. In other words, food and water supplies will be consumed over time because the objective of the regenerative LSS is to cover part of the needs of the crew, and increased production is discouraged by extra resources and efficiency terms (respectively (32) and (33)). For what concerns the two atmospheres, it is advisable, when possible, to keep their volumes stable. Thus we introduce a target volume for the smallest of the two, which is the cabin, corresponding to half its maximum volume. This target helps the system lie in an equilibrium where there is more room to maneuver the gases. With equivalent premises and considerations, we also add a mid-range target to the oxygen in the cabin, which is the only gas to be upper- and lower-bounded, see (37). With $\omega_{g_{c_5}} \in \mathbb{R}_{\geq 0}$ and $\omega_{[O_2]} \in \mathbb{R}_{\geq 0}$ the two (relatively low) weights for cabin volume and oxygen level, respectively, $W_4(t)$ in the following represent the corresponding quadratic term in the cost function:

$$W_4(t) = \omega^2_{g_{c_5}}(t)\left(\|g_{c_5}(t)\|_1 - 0.5\bar{g}_{c_5}(t)\right) + \omega^2_{[O_2]}\left(\frac{g_{c_5,[O_2]}(t)}{\|g_{c_5}(t)\|_1} - 0.21\right)^2. \tag{42}$$

Let T_s be the sampling time and assume an equally spaced sampling in prediction, that is $T(i) - T(i-1) \equiv T_s$, $i = 1, \dots, p$, recall that $x(k) \triangleq x(t + T(k))$, then

$$W_5(k) = (u(k) - (u(k-1)))^\intercal W^2_{\delta u}(u(k) - (u(k-1))) \tag{43}$$

with $W_{\delta u} \in \mathbb{R}^{n_u \times n_u}_{\geq 0}$, represents a term in the cost function that penalizes the input increments, providing a direct knob on how aggressive the behavior of the controller should be. By combining all the cost terms introduced in Section 5, we can derive the following cost function:

$$V = \frac{1}{2}\epsilon W^2_\epsilon \epsilon + \sum_{k=0}^{p-1} W_2(k) + W_3(k) + 0.5W_5(k) + \sum_{k=1}^{p} W_1(k) + \frac{1}{2}W_4(k) \tag{44}$$

where $\epsilon \in \mathbb{R}^{n_\epsilon}_{\geq 0}$ is the vector of *slack variables*, and $W_\epsilon \in \mathbb{R}^{n_\epsilon \times n_\epsilon}_{\geq 0}$ the corresponding weight matrix. Typically, all the constraints defined on system states are softened by introducing slack variables which are highly penalized in the cost function and avoid infeasible optimization problems. The requirements elaborated in Sections 5.6 and 5.7 are defined as function of one or more states, and therefore are all softened. Details on the specific softening strategy we adopted in the tests are given in Section 6.

Summarizing, at each time-step, given the sequence of parameters:

$$\Theta = \begin{bmatrix}\theta(t) & \theta(t+T(1)) & \dots & \theta(t+T(p-1))\end{bmatrix} \tag{45}$$

the MPC controller minimizes V in (44) with respect to the sequences of inputs:

$$U = \begin{bmatrix}u(t) & u(t+T(1)) & \dots & u(t+T(p-1))\end{bmatrix} \tag{46a}$$

and slack variables $\epsilon(t)$ over a series of p prediction steps, and subject to the equality constraints on the system dynamics (1) (which are built according to Section 4), and subject to the inequality constraints from Eqs. (34) to (41). The optimization problem takes into account the future evolution, when known, of quantities $\theta(t)$ that affect the prediction model and of the cost function and constraints (for instance, time-varying requirements). This is often referred to as *anticipative action*, which makes MPC highly valuable in the context of supervisory control for regenerative LSS, where the future evolutions of such factors are often well determined and scheduled.

5.9. Materials and methods

The simulation model, implementing the generic state-update differential equation (1), has been entirely developed in MATLAB® R2022a. As with the formulation, the implementation also emphasizes modularity so that more accurate mechanistic models for the compartments could be integrated, and so that the network connections can be easily updated. MATLAB code has been preferred over Simulink to favor portability of the models. The implementation of the network model supports code generation for faster simulations with compiled code. The MPC controller is implemented with *ODYS Embedded MPC* v3.6.0, a software tool that provides efficient MPC and state estimation functions for real-time applications in library-free *C* code, crafted with emphasis on execution speed, numerical robustness, and limited memory footprint (ODYS, 2019). *ODYS Embedded MPC* provides interfaces to MATLAB.

6. Simulation of the regenerative LSS during a mission

In this section, we present numerical closed-loop results for the operation of the entire MELiSSA loop over the course of a mission, where the coordination of the whole regenerative LSS is handled by a single supervisory MPC that manipulates a total of $n_u = 16$ actuators, see (29). The MPC formulation is the one described in Section 5, and the nonlinear model of the network is detailed in Section 2. The nominal values for the parameters $\theta(t)$, normalized for a single crew member, are collected in Table 4 and correspond to a nominal situation (Anderson et al., 2015). All the parameters can vary over time, as, for instance, the amount of food, water and oxygen is function of the caloric expenditure due to different activities performed by the crew. Similarly, the diet can follow a rotation schedule and is subject to changes that can depend on crew's health. For the sake of example scenarios tested here, only the crew need for O_2, which affects the fastest dynamics, is time-varying, and its profile during the course of a day is depicted in Fig. 6. In order to avoid infeasible optimization problems, a different slack variable is introduced for each constraint type (i.e. all the realizations of the same constraint in prediction share the same slack variable). This translates into a total of $n_\epsilon = 12$ slack variables. All the additional resources collected by $\rho(t)$ in Eq. (30) are enabled and usable by the controller. The sampling time for the MPC controller has been set to $T_s = 0.1$h and the prediction horizon is 1h, from which we have $p = 10$ prediction steps. The sensitivities (25) are recomputed at each prediction step, and they are obtained through finite differences. The max iteration number for the SQP algorithm is set to three, meaning that up to three QP problems are solved at every MPC instance. With this setup, the prediction model has $n_x = 227$ states and $n_u = 16$ manipulated inputs, resulting in an optimization problem with 172 variables and 560 inequality constraints.

We simulate the first 56 days of a space mission with one crew member, which is enough to appreciate the evolution to a steady state of the different subsystems and evaluate the circularity of the network. Food and water tanks have a capacity of 5000 mol and are initially filled at the maximum and half capacity, respectively. The atmospheric volumes are 2770 mol for the greenhouse and 820 mol for the cabin crew, both initially filled at half capacity. Fig. 7 shows the quantities related to safety and survivability, as described in Section 5.7. It is important to stress that in the considered MPC setup, there is no reward

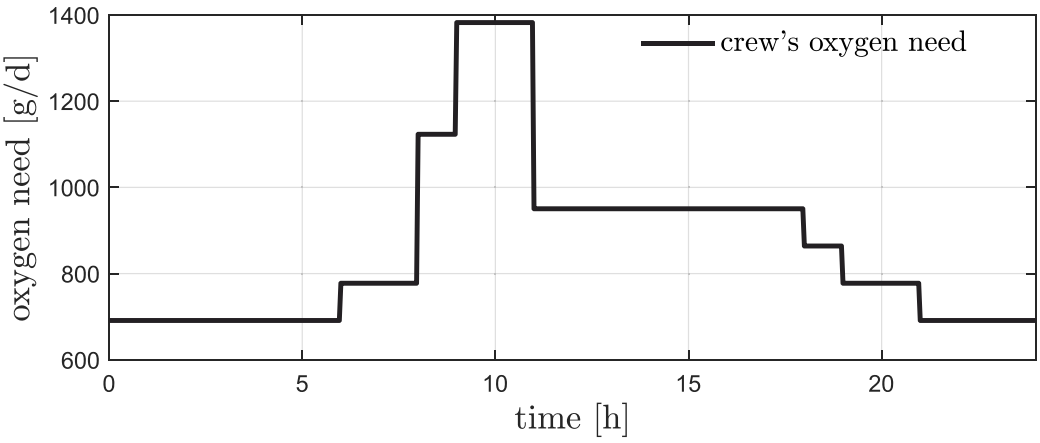

Fig. 6. Time varying O_2 needs of the crew during the course of a day, normalized for one crew member. In the simulation scenario, the needs are equal for all the days of the mission.

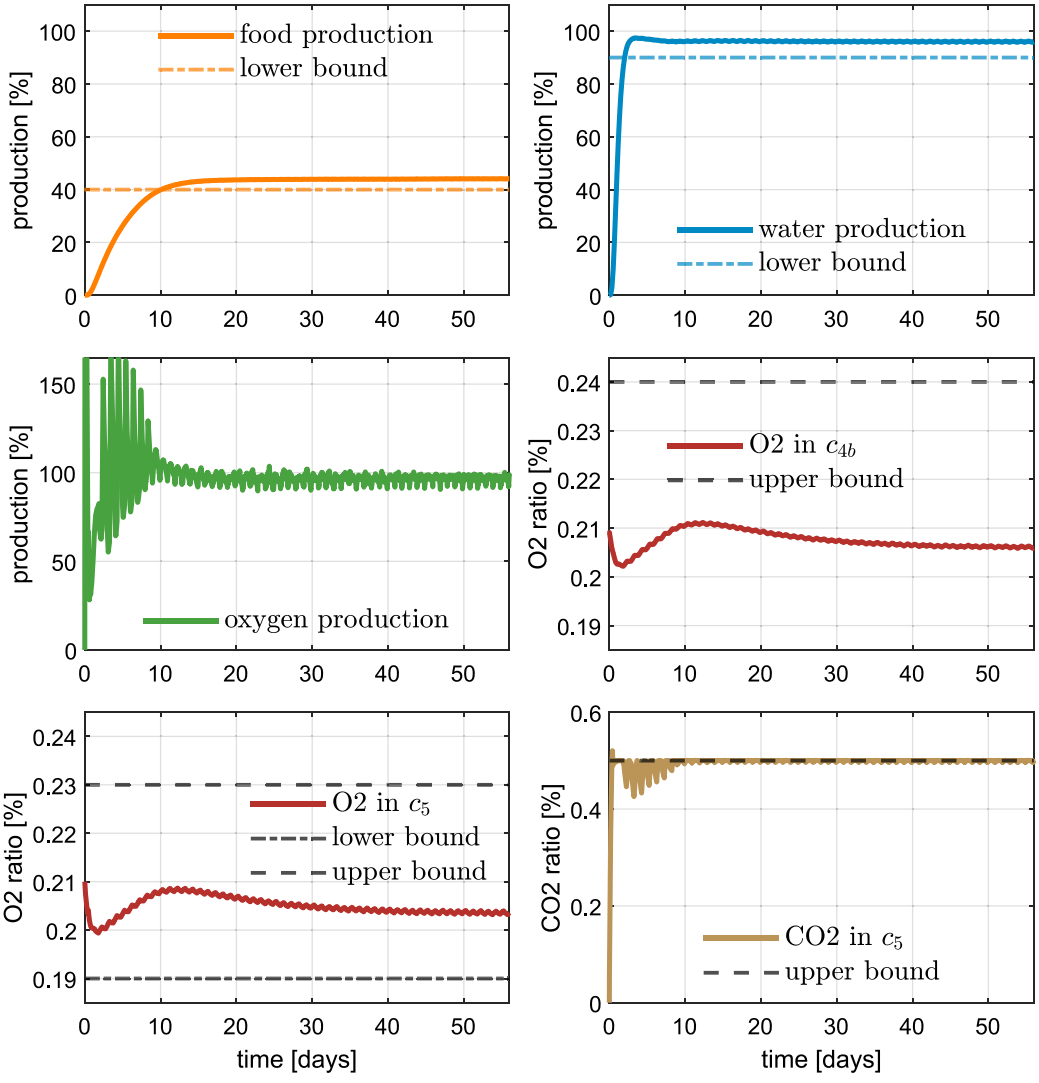

Fig. 7. Results measured by performance metrics for the regenerative LSS related to safety and survivability. For space reasons, constraint (41) is not shown as, besides the initial transient, the maximum ammonia ratio over the simulation is 0.05%, well below the 0.2 bound.

for increased production, as a preliminary objective of the study is to evaluate the autarky of the system, comparing different architectures. However, $V(t)$ could very easily include such a term, leading to a trade-off between the use of extra resources and the amount of produced food and water. Nonetheless, Fig. 7 shows that the current formulation is able to honor all the safety/survivability constraints for the tested architecture. That is achieved by manipulating the control inputs as shown in Fig. 8, which collect the time evolution of the subset of $u(t)$

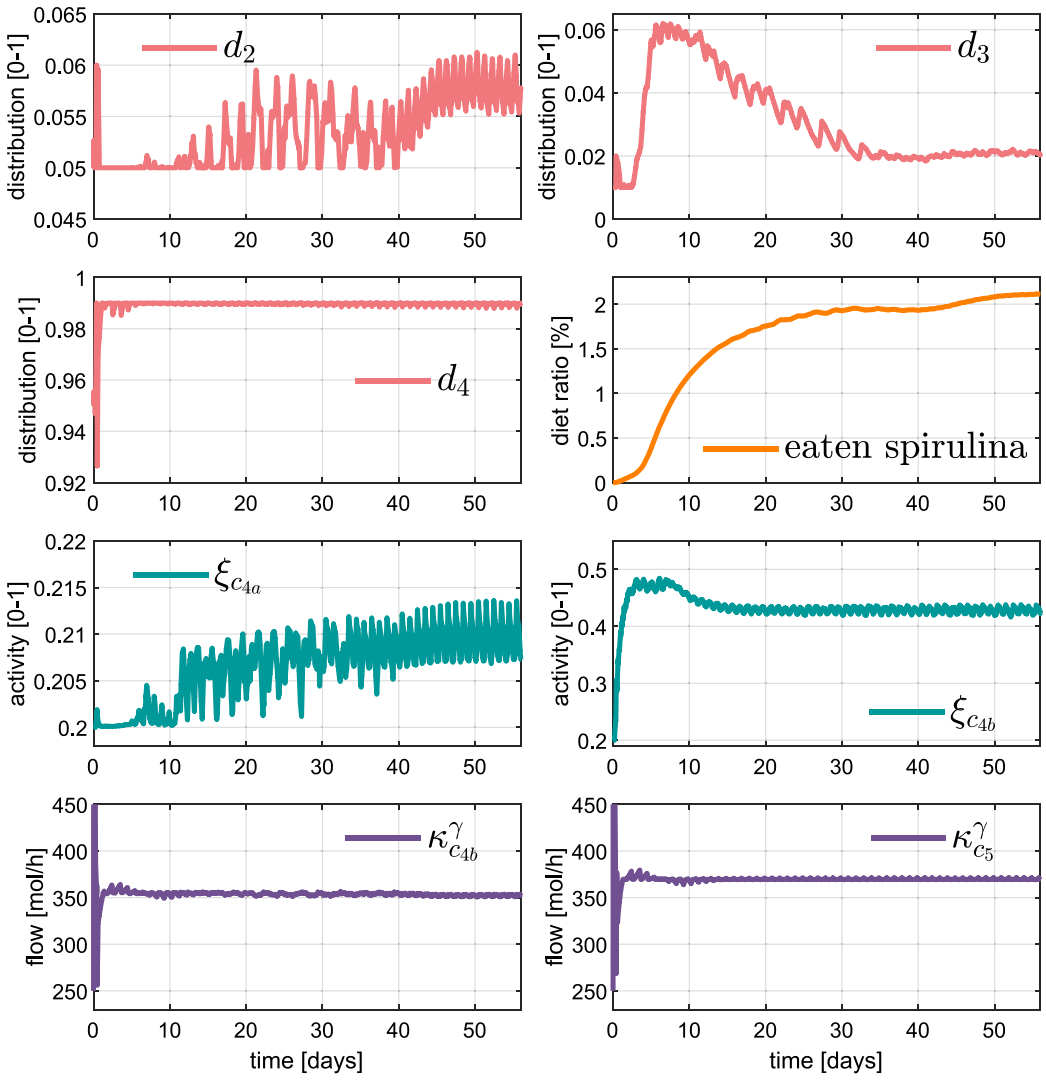

Fig. 8. Subset of $u(t)$ including distributors, compartments activities and manipulated flows. The figure shows only those distributors that in this scenario have a non-constant value. Indeed $d_1(t) = d_5(t) = 1, \forall t$ holds, meaning that all the waste passes by c_1, and that all the spirulina produced is being eaten. The orange line shows the percentage of spirulina in the crew diet, which is well below the 5% toxicity bound.

Table 3
Cumulative mass of un-recyclable waste produced during the first 56 days of the mission.

Component	Phase	Waste (kg)
C1 biomass	S	0.6992
Non-degraded organic matter	S	10.2333
Dihydrogen	G	1.4178

that does not contain the additional resources $\rho(t)$. Distributors d_1 and d_5 assume consistently the value $d = 1$ over the entire experiment, so they are not shown. In short, that means that all the waste passes by c_1, for possible transformation before eventually being sent to the waste storage and that all the produced spirulina is eaten by the crew. The orange plot on eaten spirulina in Fig. 8 shows that its toxicity threshold in crew diet (5%, Eq. (27)) is not violated. The usage of extra resources, more precisely the subset of $\rho(t)$ that is not identically zero during the experiment, is shown in Fig. 9. It is interesting to note that all the injection points for H_2SO_4 are exploited, whereas for H_3PO_4 only one is used. The proposed framework proves to be useful in designing the network architecture, by taking into account the dynamical model of the circular system operating according to an optimal control policy.

Lastly, the quantities that affect the terms $W_1(t)$ and $W_2(t)$, according to Eqs. (31) and (32) are reported in Fig. 10. It is evident that there exists an initial transient in which more chemical elements are needed for a faster startup of the chemical reactions in the compartments. After that, the mass of extra resources being utilized stabilizes in the timeframe of a week. Conversely, the produced waste reaches a steady-state value only after approximately three weeks, dynamics that are dominated by solid timescale. At the end of the 56 days, the cumulative mass of un-recyclable waste produced is 12.35 kg, whereas the mass of extra resources consumed is 2 kg. Table 3 details the waste composition after the first 56 days of the mission in terms of C1 biomass, non-degraded organic matter and dihydrogen. Lastly, it is worth stressing that the needs of food, water, and oxygen of the crew, and the need for carbon dioxide of the higher plants, are 100% satisfied by the controlled system thanks to the correct manipulation of the storage systems and extra resources. If we consider the nominal values of Table 4, this means that in the 56 days mission the crew requires approximately 37 kg of food, 168 kg of water and 48 kg of oxygen. The higher plants require instead, approximately, 65 kg of CO_2.

Next, we test the proposed framework in the presence of a failure. MPC is particularly suited to handle faulty scenarios, as an easy re-configuration is achieved by modifying the prediction model and/or constraints according to the change in the dynamics induced by the

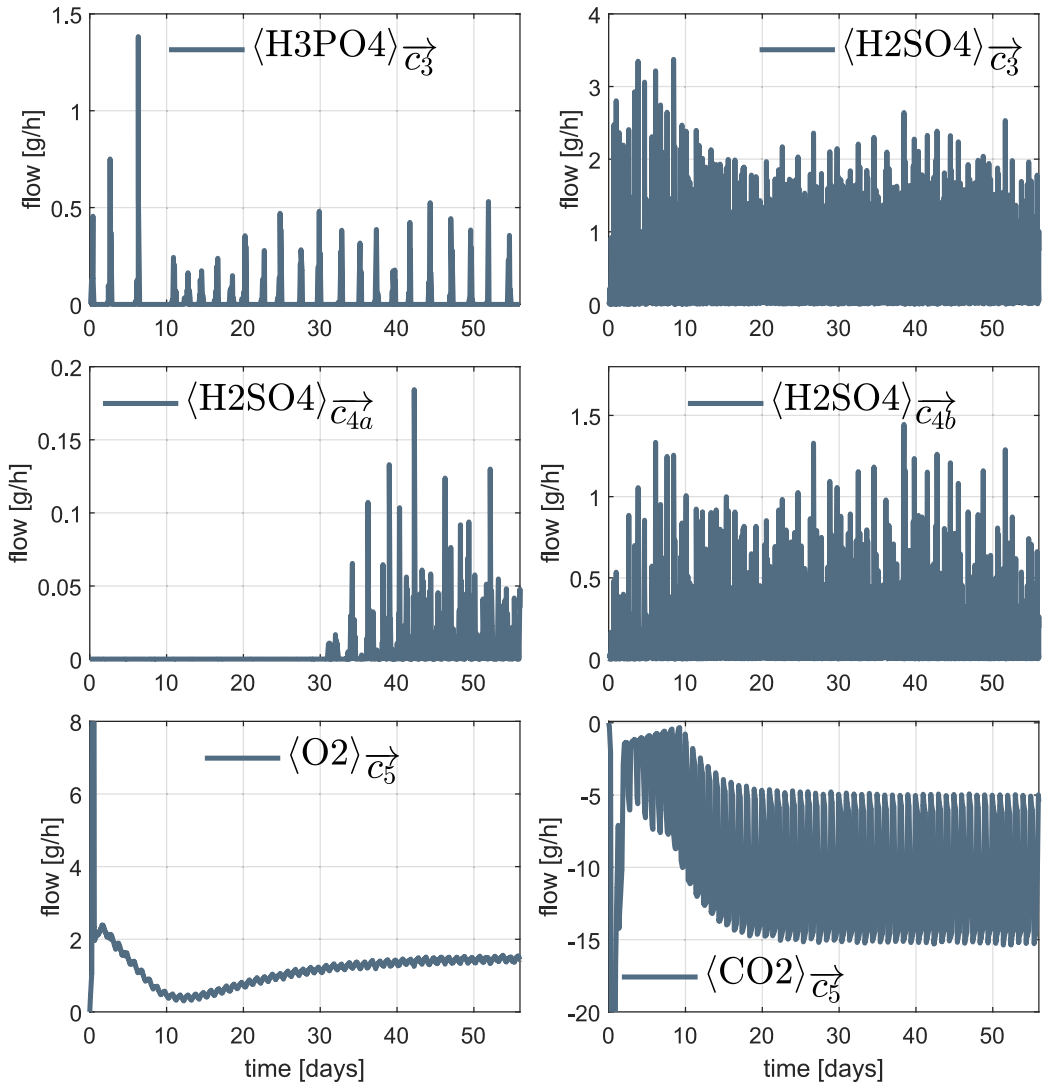

Fig. 9. Extra resources manipulated by the MPC controller, see $\rho(t)$ according to Eq. (30). This figure shows only the ones that are different from zero, namely the ones MPC discovers necessary to honor constraints while minimizing $V(t)$. The bottom right plot represents the CO_2 extracted which is part of the $W_1(t)$ cost function term.

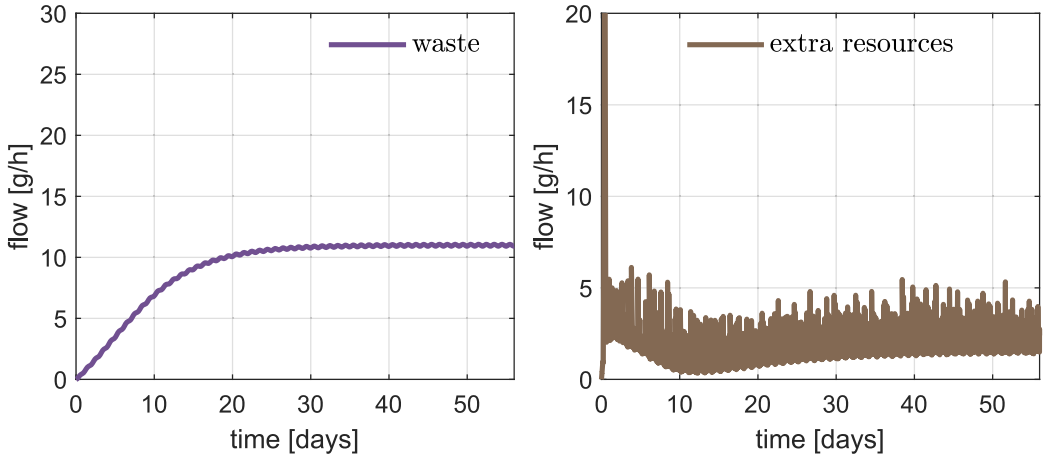

Fig. 10. Total waste that cannot be recycled (on the left) and total extra resources injected into the system (on the right) during the experiment, which affect terms (31) and (32) in the MPC cost function. The total waste on the left does not include the CO_2 removed from the cabin, which is instead shown in Fig. 9.

fault. Moreover, in the presence of anomalous scenarios, the control objectives (and their priority) might be redefined, and that is seamlessly achieved by modifying the terms in the cost function. Maintenance stops, failures, and nominal efficiency drops in a compartment are typical events that the supervisor control should handle by preserving the system operation and optimizing the time to recovery. In this study,

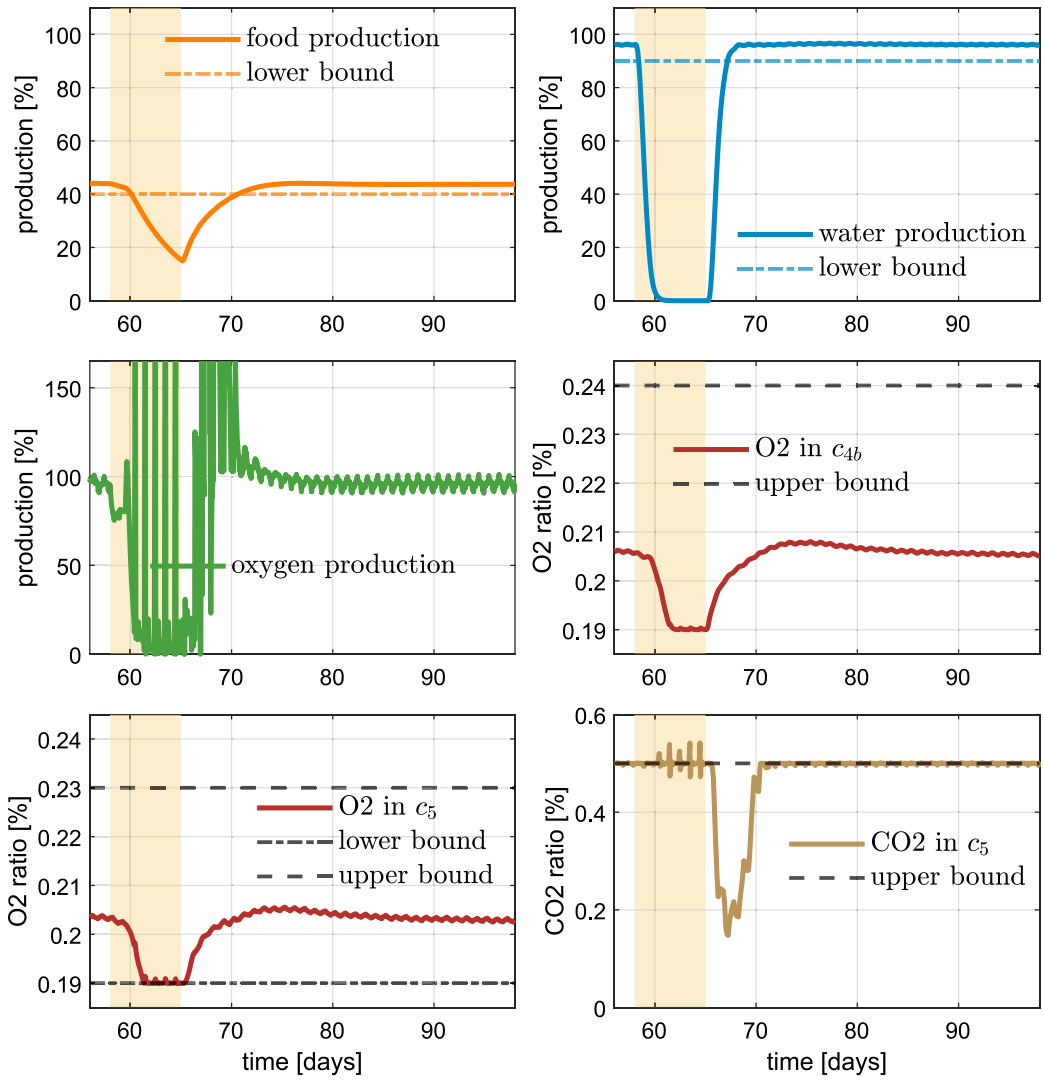

Fig. 11. Results measured by performance metrics for the regenerative LSS related to safety and survivability in the failure scenario. The period of crew sickness is highlighted with the yellow patch and lasts for 7 days.

Table 4
Nominal values for parameters $\theta(t)$ normalized for a single crew member. In the test scenario $\langle O_2 \rangle_{c.}$ is time-varying and its daily evolution shown in Fig. 6.

Parameter	Nominal value
$\bar{f}$	667 g/d
$\mathcal{D}_{\text{proteins}}$	(122 g/d)/$\bar{f}$
$\mathcal{D}_{\text{lipids}}$	(103 g/d)/$\bar{f}$
$\mathcal{D}_{\text{carbohydrates}}$	(405 g/d)/$\bar{f}$
$\mathcal{D}_{\text{nucleic}}$	(0 g/d)/$\bar{f}$
$\mathcal{D}_{\text{eps}}$	(0 g/d)/$\bar{f}$
$\mathcal{D}_{\text{fibers}}$	(37 g/d)/$\bar{f}$
$\langle H_2O \rangle_{c.}$	3000 g/d
$\langle O_2 \rangle_{c.}$	864 g/d
$\langle CO_2 \rangle_{p.}$	1160 g/d

we test a situation in which the crew suddenly gets sick. The scenario we are testing follows in time (and with the same architecture) the simulation of Figs. 7 to 9, it can indeed be considered as a continuation of the same mission, for additional 42 days. While the crew is sick, the solid and liquid output flow of c_5 is considered waste that cannot be recycled (to contain the contamination) and is therefore sent to the waste storage, exiting the circular system. This translates into the following simple modifications to the MPC prediction model (Eqs. (47a) and (47b)) and to its cost function (Eq. (47c)):

$$\delta_1 = \sigma_{c_2} + \sigma_{c_3} + (\sigma_{c_{4a}} - \bar{f}_s \circ \frac{1}{24 m_s}) + \text{NEP}(\sigma_{c_{4b}}) \tag{47a}$$

$$\boldsymbol{\Phi}^t_{c_1}(t) = \begin{bmatrix} \delta_1(t) d_1(t) \\ \lambda^{\ell}_{c_{4a}}|_{H_2O=0}(t) + \lambda^{\ell}_{c_{4b}}|_{H_2O=0}(t) \\ \mathbf{0}_{n_g} \end{bmatrix} \tag{47b}$$

$$\begin{aligned} W_1(t) = {} & \left(m_s \circ \omega_\sigma(t)\right)^{\intercal} \left(\delta_1(t)(1 - d_1(t)) + \sigma_{c_5}(t)\right) + \left(m_\ell \circ \omega_\lambda(t)\right)^{\intercal} \lambda_{c_5}(t) \\ & + \left(m_g \circ \omega_\gamma(t)\right)^{\intercal} \left(H_2(\gamma_{c1}(t)) + H_2(\gamma_{c2}(t))\right) \\ & + m_{[CO_2]} \omega_{CO_2}(t) \max(0, -\langle CO_2 \rangle_{\overrightarrow{c_5}}(t)) \end{aligned} \tag{47c}$$

where we have introduced the weights ω_λ for liquid waste, absent before, and $\omega_{\lambda,i}(t) = \omega_{\gamma,j}(t)$, $\forall i \in \{1, \dots, n_\ell\}$, $\forall j \in \{1, \dots, n_g\}$, $\forall t > t_0$. Note that Eqs. (47) are the only modifications to the MPC formulation that are needed to optimally handle crew sickness, while the rest remains unchanged. The overall system under this failure scenario has been tested, and the results are shown in Figs. 11–13. The crew gets sick on day 58, and this condition lasts for 7 days. This time frame is highlighted with a yellow background in the figures.

We note that the weights of the controller have not been altered with respect to the nominal scenario. A time-varying tuning dedicated to the occurrence of specific situations, or phases of the mission, may

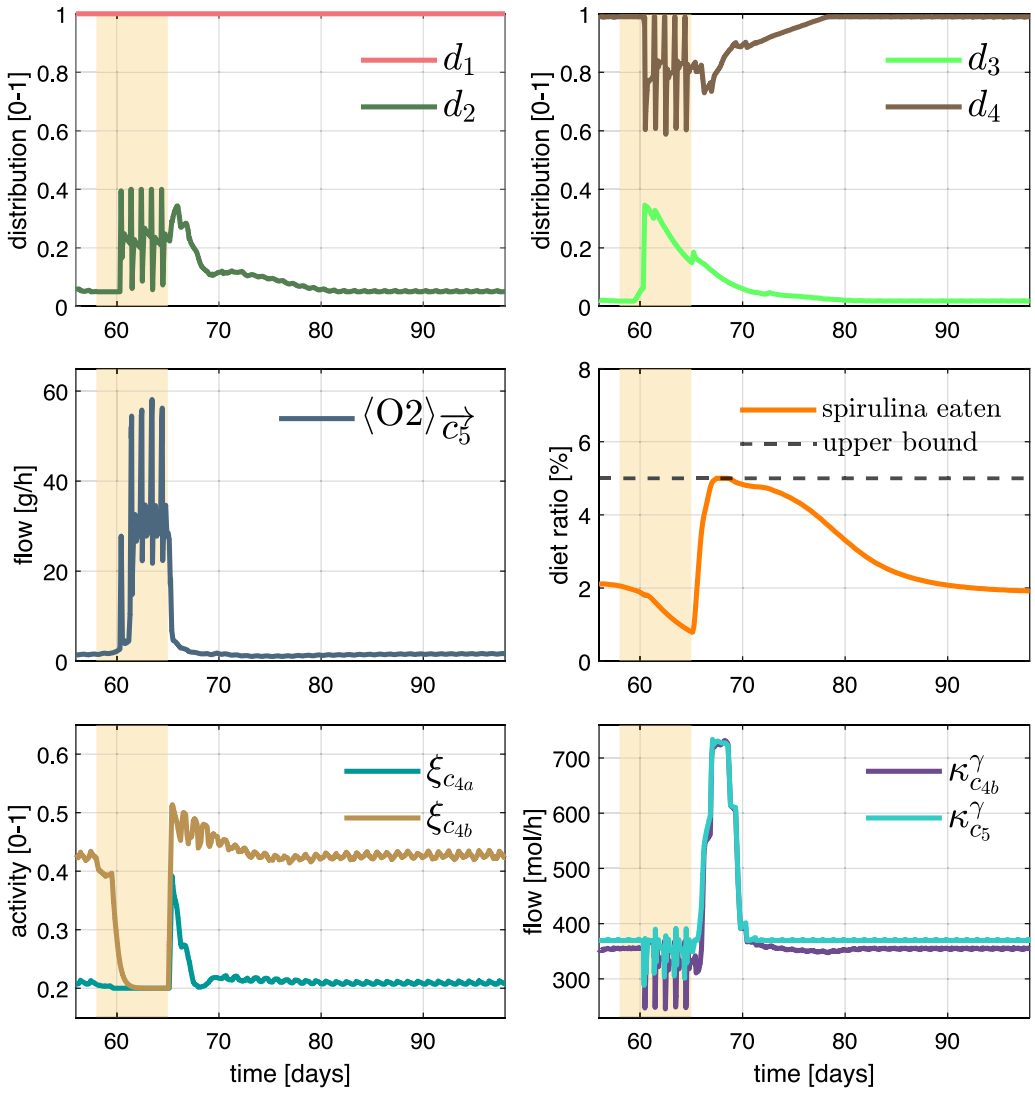

Fig. 12. Subset of $u(t)$ including distributors, compartments activities, and manipulated flows. The period of crew sickness is highlighted with the yellow patch and lasts for 7 days.

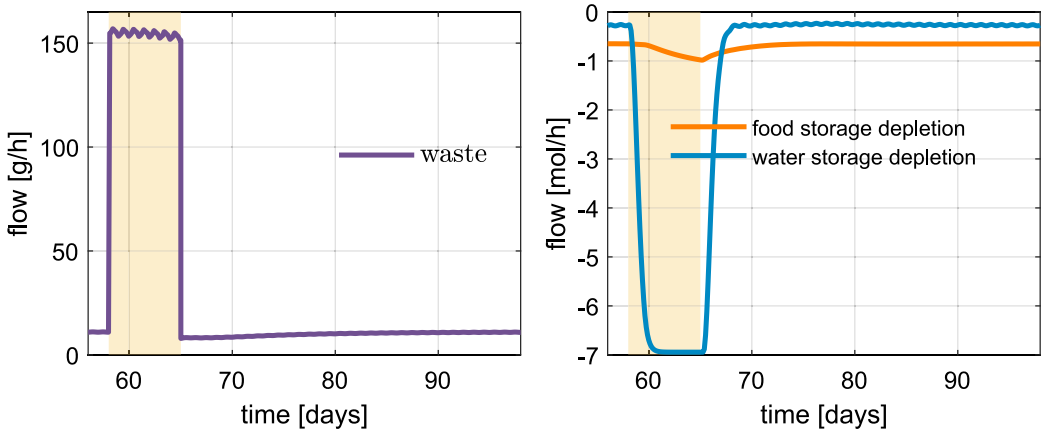

Fig. 13. Total waste that cannot be recycled (on the left) and depletion of food and water storages (on the right) during a failure scenario. The period of crew sickness is highlighted with the yellow patch and lasts for 7 days.

offer superior performance and would be easily implemented with the proposed MPC controller. It is interesting, however, to note that, without any tuning modification, the controller is perfectly capable of handling the faulty situation, proving the proposed framework to be a

valid tool to quickly investigate different scenarios and architectures. While the crew is sick, c_{4a} and c_{4b} miss necessary elements for their chemical processes, and therefore the production of food, water, and oxygen drops below their respective targets (see Fig. 11). The crew needs are, however, always 100% met, as food and water are taken from the storage systems (note in Fig. 13 the increased depletion rate of both storages for the fault duration), while the oxygen is supplied with a buffer storage directly manipulated by MPC (third plot of Fig. 12). Fig. 13 also shows the increased waste production during sickness time. Excluding production target, all other constraints that concern safety, storage, and actuator bounds are respected. After the sickness period is over, the system goes back to normal operation. It is interesting to note that, in order to speed up the process, the controller includes more spirulina in the crew diet for a certain amount of time, while still honoring its toxicity upper bound. This test has highlighted how the architecture considered here has no means to maintain a positive production rate while the products of c_5 are wasted. This may trigger an investigation on a different set of buffer storages, see Eq. (30), that could supply c_{4a} and c_{4b} during that time.

The modeling/control mathematical framework and its implementation in the simulation environment are validated through the computation of mass balances, elaborating the point-wise composition of mass in the entire system in terms of the chemical elements that characterize components in Table 1, namely carbon, hydrogen, oxygen, nitrogen, sulfur and phosphorus. Such computation encompasses the status of tanks, use of additive resources, volumes, and non-expired flow dynamics. The result over the course of the experiment is a worst-case deviation, element-wise, of 0.02% of mass with respect to the initial composition, confirming the correctness of the closed-loop setup.

Even though the purpose of the paper is not to prove the feasibility of the approach on the embedded computational units that might be used in a real mission, we provide here some information about the execution time and memory occupancy of the designed controller. Despite the complexity of the problem formulation, the controller is easily implementable in real time with state-of-the-art software like *ODYS Embedded MPC*, which shows a maximum execution time of as little as 55 ms on a 12th Gen Intel® Core™ i9-12900H @2.50 GHz. This is orders of magnitude smaller than the 6 min sampling time, providing ample margins for using less powerful computing hardware and/or increasing the complexity of the design, for example, by including mechanistic models and additional requirements. Memory-wise, *ODYS Embedded MPC* implementation is also very efficient, allocating only about 2.5 MB of data for the considered problem.

7. Conclusion

In this study, an MPC methodology for the global control of a circular life support system was developed and preliminary investigated using the MELiSSA loop as a test case. This investigation aimed to validate a first implementation of an advanced supervisory controller for a complete circular life support system, focusing on demonstrating the stability of the loop before optimizing it. A preliminary dynamical simulation of a MELiSSA loop architecture considering all the compartments connected in all the phases was developed. The ability of the MPC controller to satisfy numerous requirements and constraints elaborated by the MELiSSA project has been demonstrated. The controller was able to satisfy all the requirements throughout a full mission scenario of 98 days. The capacity of MPC to react to undesired situations was also proven by analyzing a crew sickness scenario. By cleverly exploiting the different available degrees of freedom, the controller was still able to honor all the requirements and constraints. Suggestion for future work include the addition of survivability requirements for the microalgae, and the investigation of a hierarchical topology of the supervisory MPC (Scattolini, 2009), with levels corresponding to different phases so as to better exploit prediction capabilities. Furthermore, anticipative actions could be included, thus exploiting available information on the crew's, and, more generically, mission's schedule to enhance control performance.

CRediT authorship contribution statement

Gionata Cimini: Writing – original draft, Software, Methodology, Conceptualization. **Marco Gatti:** Writing – original draft, Validation, Data curation. **Daniele Bernardini:** Writing – review & editing. **Alberto Bemporad:** Writing – review & editing. **Chloé Audas:** Writing – review & editing, Supervision. **Claude-Gilles Dussap:** Writing – review & editing.

Declaration of competing interest

The authors declare that they have no known competing financial interests or personal relationships that could have appeared to influence the work reported in this paper.

Acknowledgment and funding

This activity has been performed in the frame of the MELiSSA Memorandum of Understanding (ESA 4000100293) and funded by the European Space Agency's Exploration Preparation Research and Technology (ExPeRT) Program, within the Terrae Novae European Exploration Envelope Program (E3P). For more information regarding the MELiSSA foundation please visit https://www.melissafoundation.org/.

References

Alemany, L., Peiro, E., Arnau, C., Garcia, D., Poughon, L., Cornet, J.-F., Dussap, C.-G., Gerbi, O., Lamaze, B., Lasseur, C., Godia, F., 2019. Continuous controlled long-term operation and modeling of a closed loop connecting an air-lift photobioreactor and an animal compartment for the development of a life support system. Biochem. Eng. J. 151, 107323.

Anderson, M.S., Ewert, M.K., Keener, J.F., Wagner, S.A., 2015. Life support baseline valuesand assumptions document. Number: NASA/TP-2015-218570.

Audas, C., Ortega Ugalde, S., Paille, C., Lamaze, B., Lasseur, C., 2022. Life support systems beyond low earth orbit advocates for an improved resources management approach. Ecol. Eng. Environ. Prot. 2022, 5–13.

Begon, M., Townsend, C.R., 2021. Ecology: From Individuals to Ecosystems. John Wiley & Sons.

Bemporad, A., Bernardini, D., Long, R., Verdejo, J., 2018. Model predictive control of turbocharged gasoline engines for mass production. SAE Tech. Pap. 2018-01-0875.

Binois, C., Lasseur, C., Cornet, J.F., Doyle, D., 1994. Model based predictive control of MELISSA photobioreactors. Steady state determination. SAE Trans. 103, 1029–1037.

Brunet, J., Gerbi, O., André, P., Davin, E., Avezuela Rodriguez, R., Carbonero, F., Soumalainen, E., Lasseur, C., 2010. Alisse : Advanced life support system evaluator. In: 38th COSPAR Scientific Assembly. vol. 38, p. 2.

Cimini, G., Bemporad, A., Bernardini, D., 2017. ODYS QP solver. ODYS S.r.l. (https://odys.it/qp).

Cimini, G., Bernardini, D., Levijoki, S., Bemporad, A., 2021. Embedded model predictive control with certified real-time optimization for synchronous motors. IEEE Trans. Control Syst. Technol. 29 (2), 893–900.

Ciurans, C., Bazmohammadi, N., Poughon, L., Vasquez, J.C., Dussap, C.G., Gòdia, F., Guerrero, J.M., 2022. Hierarchically controlled ecological life support systems. Comput. Chem. Eng. 157, 107625.

Ciurans, C., Bazmohammadi, N., Vasquez, J.C., Dussap, G., Guerrero, J.M., Godia, F., 2021. Hierarchical control of space closed ecosystems: Expanding microgrid concepts to bioastronautics. IEEE Ind. Electron. Mag. 15 (2), 16–27.

Cornet, J.-F., Dussap, C.G., Leclercq, J.-J., 2002. Simulation, design and model based predictive control of photobioreactors. In: Hofman, M., Thonart, P. (Eds.), Engineering and Manufacturing for Biotechnology. Springer Netherlands, Dordrecht, pp. 227–238.

Dussap, C.-G., Cornet, J.-F., Gros, J.-B., 1993. Simulation of mass fluxes in the MELISSA microorganism based ecosystem. In: International Conference on Environmental Systems. SAE International.

Fahrion, J., Mastroleo, F., Dussap, C.-G., Leys, N., 2021. Use of photobioreactors in regenerative life support systems for human space exploration. Front. Microbiol. 12.

Falcone, P., Borrelli, F., Tseng, H.E., Asgari, J., Hrovat, D., 2008. Linear time-varying model predictive control and its application to active steering systems: Stability analysis and experimental validation. Internat. J. Robust Nonlinear Control 18 (8), 862–875.

Franchi, L., Feruglio, L., Mozzillo, R., Corpino, S., 2018. Model predictive and reallocation problem for CubeSat fault recovery and attitude control. Mech. Syst. Signal Process. 98, 1034–1055.

Fulget, N., Poughon, L., Richalet, J., Lasseur, C., 1999. MELISSA: Global control strategy of the artificial ecosystem by using first principles models of the compartments. Adv. Space Res. 24 (3), 397–405.

Gitelson, I., Terskov, I., Kovrov, B., Sidko, F., Lisovsky, G., Okladnikov, Y., Belyanin, V., Trubachov, I., Rerberg, M., 1976. Life support system with autonomous control employing plant photosynthesis. Acta Astronaut. 3 (9), 633–650.

Hendrickx, L., Mergeay, M., 2007. From the deep sea to the stars: Human life support through minimal communities. Curr. Opin. Microbiol. 10 (3), 231–237.

Lasseur, C., 2008. Melissa: The European project of a closed life support system.

Lasseur, C., Verstraete, W., Gros, J., Dubertret, G., Rogalla, F., 1996. MELISSA: A potential experiment for a precursor mission to the moon. Adv. Space Res. 18 (11), 111–117.

Mayne, D., Rawlings, J., Diehl, M., 2018. Model Predictive Control: Theory and Design, second ed. Nob Hill Publishing, LCC, Madison,WI.

MELiSSA Foundation, Melissa space research program. URL https://www.melissafoundation.org/page/melissa-project. (Accessed 18 December 2023).

Mergeay, M., Verstraete, W., Dubertret, G., Lefort-Tran, M., Chipaux, C., Binot, R., 1988. MELiSSA: A micro-organisms-based model for CELSS development. In: ESA, Third European Symposium on Space Thermal Control and Life Support Systems P 65-68(SEE N 89-28214 22-54).

Nelson, M., Allen, J., Ailing, A., Dempster, W., Silverstone, S., 2003. Earth applications of closed ecological systems: Relevance to the development of sustainability in our global biosphere. Adv. Space Res. 31 (7), 1649–1655.

ODYS, S., 2019. ODYS embedded MPC. (https://odys.it/embedded-mpc).

Pannico, A., Cimini, G., Quadri, C., Paradiso, R., Bucchieri, L., Rouphael, Y., De Pascale, S., 2022. A plant characterization unit for closed life support: Hardware and control design for atmospheric systems. Front. Astron. Space Sci. 9.

Poughon, L., Dussap, C.G., Gros, J.B., 1999. Dynamic model of a nitrifying fixed bed column: Simulation of the biomass distribution of nitrosomonas and nitrobacter and of transient behaviour of the column. Bioprocess Eng. 20 (3), 209–221.

Poughon, L., Farges, B., Dussap, C., Godia, F., Lasseur, C., 2009. Simulation of the MELiSSA closed loop system as a tool to define its integration strategy. Adv. Space Res. 44 (12), 1392–1403.

Poulet, L., Dussap, C.-G., Fontaine, J.-P., 2020. Development of a mechanistic model of leaf surface gas exchange coupling mass and energy balances for life-support systems applications. Acta Astronaut. 175, 517–530.

Savage, C., Tan, G., Lasseur, C., 2001. ESA developments in life support technology: achievements and future priorities. Acta Astronaut. 49 (3), 331–344.

Scattolini, R., 2009. Architectures for distributed and hierarchical model predictive control – a review. J. Process Control 19 (5), 723–731.

Schwenzer, M., Ay, M., Bergs, T., Abel, D., 2021. Review on model predictive control: An engineering perspective. Int. J. Adv. Manuf. Technol. 117 (5), 1327–1349.

Thiron, B., 2020. Global Control of a Life Support System : Flow control and optimisation (Master's thesis). KTH, School of Electrical Engineering and Computer Science (EECS).

Vermeulen, A.C.J., Papic, A., Nikolic, I., Brazier, F., 2023. Stoichiometric model of a fully closed bioregenerative life support system for autonomous long-duration space missions. Front. Astron. Space Sci. 10.